THE REGULATION OF AUTOPHAGY AND ITS ROLE IN MITOTIC EXIT

APPROVED BY SUPERVISORY COMMITTEE

Beth Levine, M.D.

Benjamin Tu, Ph.D.

Melanie Cobb, Ph.D.

Michael White, Ph.D.

DEDICATED TO MY FAMILY.

MY PARENTS, MY HUSBAND YUXIAO AND MY SWEETHEART ANGELINA.

THE REGULATION OF AUTOPHAGY AND ITS ROLE IN MITOTIC EXIT

by

ZHENYI AN

DISSERTATION

Presented to the Faculty of the Graduate School of Biomedical Sciences

The University of Texas Southwestern Medical Center at Dallas

In Partial Fulfillment of the Requirements

For the Degree of

DOCTOR OF PHILOSOPHY

The University of Texas Southwestern Medical Center

Dallas, Texas

August, 2014

ACKNOWLEDGEMENTS

I would like to thank my mentor, Dr. Beth Levine, for her support for my projects and career. Her enthusiasm and insight into science guided me through my thesis. She took every effort to train me to become a better scientist. I would also like to thank the Levine lab members, especially Dr. Yongjie Wei for his enormous help on the Beclin 1 phosphorylation project. I thank former post-doctoral fellows, Amina Tassa and Collin Thomas for initiating the yeast cell cycle project. Zhongju Zou assisted with the tumorigenesis and other animal experiments, as well as the immunofluorescence studies. Lori Nguyen helped with the mouse genotyping and breeding. I would also like to thank other Levine lab members, who provided a supportive and stimulating research environment.

I would like to thank Abhijit Bugde and Dr. Kathrine Luby-Phelps in the UTSW Live Cell Imaging core facility, and Dr. Sunil Laxman and Dr. Benjamin Tu for their help on the live cell yeast imaging work. Dr. Rui Zhong and Dr. Guanghua Xiao performed statistical analyses. I would also like to thank Dr. Daniel Klionsky, Dr. Matthias Gaestel, Dr. Tatiana Yakovleva, Dr. Denise Marciano, Dr. Zhufeng Yang, Dr. Sharon Tooze, Dr. Reuben Shaw, Dr. Martin Schmidt and Dr. Qing Zhong for providing us key reagents and technical guidance. I would like to thank my thesis committee, Dr. Benjamin Tu, Dr. Melanie Cobb, and Dr. Michael White, for their helpful suggestions on my thesis.

I want to thank my husband, Yuxiao Wang, who has provided strong support for years. Thank you for your love! I love you! I also want to thank my sweetheart Angelina, who

brings me much happiness and joy. Mom loves you so much! And also my parents, thank you so much! I could never finish this without you!

THE REGULATION OF AUTOPHAGY AND ITS ROLE IN MITOTIC EXIT

ZHENYI AN, Ph.D.

The University of Texas Southwestern Medical Center, 2014

Supervising Professor: BETH LEVINE, M.D.

Abstract

Autophagy is an evolutionarily conserved pathway in which cells enclose cytoplasmic contents in double membrane vesicles and deliver them to the lysosome for degradation. Autophagy plays critical regulatory roles in cancer, aging, neurodegeneration, immunity and many other physiological processes. Autophagy can be induced by multiple conditions such

as starvation, viral infection, exercise and oxidative stress. In this work, we studied the role of autophagy in starvation-induced cell cycle arrest and quiescence entry, and studied the function and regulation of a major phosphorylation site of Beclin 1, serine 90. In the first study, we found that the in response to starvation, autophagy-deficient yeasts failed to arrest properly in G_1/G_0, but arrested in telophase with a quiescent-specific phenotype. In a second study, we found that Beclin 1 serine 90 is a major phosphorylation site of Beclin 1, which is induced by multiple stresses such as starvation and osmotic stress. The phosphorylation of Beclin 1 serine 90 leads to the activation of autophagy and inhibition of tumorigenesis. We identified MK2/3 as kinases that positively regulate autophagy by phosphorylating Beclin 1 at amino acid residue serine 90. We also found that Beclin 1 serine 90 phosphorylation is negatively regulated by Bcl-2 and positively regulated by AMPK. Beclin 1 serine 90 phosphorylation is also important for cell survival during high osmotic stress. Taken together, these results suggest that Beclin 1 serine 90 phosphorylation is a critical event in autophagy induction, which is tightly regulated by multiple kinases and regulatory proteins.

TABLE OF CONTENTS

PRIOR PUBLICATIONS

Wang, R.C., Wei, Y., **An, Z**., Zou, Z., Xiao, G., Bhagat, G., White, M., Reichelt, J., and Levine, B. Akt-mediated regulation of autophagy and tumorigenesis through Beclin 1 phosphorylation. *Science*. 2012; 338:956-959.

He, C., Bassik, M.C., Moresi, V., Sun, K., Wei, Y., Zou, Z., **An, Z**., Loh, J., Fisher, J., Sun, Q., Korsmeyer, S., Packer, M., May, H.I., Hill, J.A., Virgin H.W., Gilpin, C., Xiao, G., Bassel-Duby, R., Scherer, P.E., and Levine, B. Exercise induced Bcl2-regulated autophagy is required for muscle glucose homeostasis. *Nature*. 2012; 481:511-515.

Wang, S., Xin, F., Liu, X., Wang Y., **An, Z.**, Qi, Q., Wang, PG. N-terminal deletion of peptide:N-glycanase results in enhanced deglycosylation activity. *PLoS One*. 2009; 4:e8335.

LIST OF FIGURES

LIST OF TABLES

LIST OF ABBREVIATIONS

AMPK	AMP-activated protein kinase
ATG	Autophagy-related gene
Beclin 1	Bcl-2 interacting coiled-coil protein 1
Bcl-X_L	B-cell lymphoma-extra large
Bcl-2	B-cell lymphoma 2
BNIP3	Bcl-2/adenovirus E1B 19 kDa protein-interacting protein 3
DAPK	Death-associated protein kinase
EGF	Epidermal growth factor
EGFR	Epidermal growth factor receptor
ER	Endoplasmic reticulum
ERK	Extracellular signal–regulated kinase
FIP200	FAK family-interacting protein of 200 kDa
JNK1	c-Jun N-terminal protein kinase 1
HMGB1	High-mobility group box 1 protein
Hsp	Heat shock protein
LC3	Microtubule-associated protein 1A/1B-light chain 3
LPS	Lipopolysaccharide
MAPK	Mitogen-activated protein kinase
MAPKAPK	Mitogen-activated protein kinase-activated protein kinase

Mcl-1	Myeloid cell leukemia protein 1
MK	Mitogen-activated protein kinase-activated protein kinase
mTORC1	Mechanistic target of rapamycin complex 1
NES	Nuclear export signal
NLS	Nuclear localization signal
PAS	Pre-autophagosomal structure
PE	Phosphatidylethanolamine
PKA	Protein kinase A
PI3K	Phosphatidylinositol 3-kinase
TIP60	60 kDa trans-acting regulatory protein of HIV type 1-interacting protein
Tsc1	Tuberous sclerosis 1
Ulk1	Unc-51-like autophagy activating kinase

CHAPTER ONE

Introduction

I. Introduction to autophagy

Autophagy is a highly conserved pathway in which cytoplasmic contents are degraded and recycled in response to stressors. Autophagy is important for maintaining cellular energy homeostasis in development and nutrient starvation. It is also critical for clearing damaged organelles, protein aggregates and intracellular pathogens. Therefore, autophagy is usually a pro-survival pathway although autophagic cell death has been reported. Autophagy plays important roles in different physiological and pathological processes such as aging, cancer, infection, inflammation and cell growth (Levine and Kroemer, 2008). Autophagy can be either selective or non-selective in removing protein aggregates and organelles (Glick et al., 2010). Understanding the signaling pathways and underlying mechanisms regulating autophagy is important for finding novel targets for disease control.

Autophagy is classified into three subtypes: macroautophagy, microautophagy and chaperone-mediated autophagy. Macroautophagy requires formation of double-membrane structures called autophagosomes to enclose cytoplasmic contents and deliver them to the lysosome for degradation. In microautophagy, the lysosome directly takes up cytoplasmic cargos for degradation. In chaperone-mediated autophagy, chaperone proteins and lysosomal

receptors facilitate lysosomal delivery of the cargos (Glick et al., 2010). We mainly focused on macroautophagy (henceforth referred to as 'autophagy') in this study.

The core autophagy machinery

As shown in **Fig. 1. 1** (Green and Levine, 2014), when autophagy is induced, an isolation membrane forms and expands to engulf intracellular cargos. The expanded double-membrane structure eventually forms an autophagosome and fuses with the lysosome. Cargos are degraded inside the autolysosome and nutrients are recycled. The autophagy-related genes (*Atg*'s) are a set of evolutionarily conserved genes required for the execution of this pathway. Most of the *Atg* genes were first discovered through genetic screens in the budding yeast *Saccharomyces cerevisiae*. More than 30 different autophagy-related genes have been identified via genetic screens in yeast and many of them are conserved in higher eukaryotes (Glick et al., 2010). The core yeast autophagy machinery can be divided into four major subgroups described as follows (Chen and Klionsky, 2011):

<u>The Atg1-Atg13-Atg17 serine/threonine kinase complex</u>

ATG1 was the first identified *Atg* gene in *S. cerevisiae*. The gene product Atg1 is a Ser/Thr kinase. Atg1 forms a complex with other proteins, which is crucial for the initiation step of autophagy. In the budding yeast, the Atg1 complex includes Atg1, Atg13 and Atg17-Atg31-Atg29 (Chen and Klionsky, 2011). The Atg1 complex also mediates the retrieval of Atg9 from the pre-autophagosomal structure (PAS) (Feng et al., 2014). In mammalian cells, this

complex is composed of Ulk1 and Ulk2 (Atg1 orthologs), Atg13 and FIP200 (**Fig. 1. 1**). Ulk1 phosphorylates Beclin 1, the mammalian ortholog of Vps30/Atg6 (Russell et al., 2013). Atg13 and Atg17 are required for the optimal kinase activity of Atg1 (Kabeya et al., 2005).

The PI3K complexes

The class III PI3K complex is essential for the formation of the isolation membrane (also known as the phagophore). In the budding yeast, there are two class III PI3K complexes: complex I and complex II (Feng et al., 2014). Components of complex I include Vps34, the PI3-kinase, Vps30/Atg6, Atg14, Atg38 and a regulatory kinase Vps15. Vps30/Atg6 directly interacts with Atg14 and is essential for autophagy (Obara and Ohsumi, 2011). Complex II includes Vps34, Vps30/Atg6, Vps38 and Vps15. Complex I is localized at the PAS and is important for recruiting PI3P binding proteins (Feng et al., 2014). In mammalian cells, the core components of the class III PI3K complex are VPS34, Beclin 1 (Vps30/Atg6 ortholog) and PIK3R4 (Vps15 ortholog). Beclin 1 is critical for PI3P synthesis and the association of the complete class III PI3K complex (Wirth et al., 2013). The core components are present in at least three different complexes: the Atg14 complex, the UVRAG complex and the Rubicon complex (Feng et al., 2014). The ATG14 complex contains Atg14 and is regulated by the interaction of Beclin 1 with Bcl-2 and AMBRA1. The UVRAG complex contains UVRAG and its regulatory protein SH3GLB1. It participates in endocytosis and autophagy. The Rubicon complex contains Rubicon, which inhibits autophagy and endosomal maturation (Feng et al., 2014).

The Atg9 complex

In the budding yeast, Atg9 is a transmembrane essential for autophagy. It recruits Atg proteins and organizes the pre-autophagosomal structure (PAS) (Webber and Tooze, 2010). Atg9 transits between the PAS and peripheral sites (Feng et al., 2014). Localization of Atg9 to the PAS requires Atg11, Atg23 and Atg27. Localization of Atg9 to the peripheral sites requires Atg1-Atg13, Atg2 and Atg18 (Feng et al., 2014). Atg1 phosphorylates Atg9 and this phosphorylation is required for autophagy (Papinski et al., 2014). The function of Atg9 is conserved in mammalian cells. Atg9A and Atg9B are the orthologs of yeast Atg9. They localize to the *trans*-Golgi network and late endosomes under nutrient-rich condition. Ulk2, WIPI2 (Atg18 ortholog) and Vps34 are required for the function of Atg9 (Feng et al., 2014).

The two ubiquitin-like protein conjugation complexes

In budding yeasts, the vesicle elongation step of autophagy involves two ubiquitin-like protein systems, the Atg8 and Atg12 systems. In the Atg8 system, the C-terminal arginine residue of Atg8 is cleaved by the cysteine protease Atg4 (Kirisako et al., 2000). Atg8 is covalently conjugated to phosphatidylethanolamine (PE) through Atg7 and Atg3. In mammals, there are multiple orthologs of yeast Atg8. They are classified into two subfamilies: the LC3 subfamily and the GABARAP subfamily (Feng et al., 2014). The LC3 subfamily proteins function in the phagophore elongation step. During autophagy, LC3-II, the lipidated form of LC3 is recruited to the autophagosomal membrane. LC3-II is the only known protein that stably associates with autophagosomes and it is commonly used as an autophagosomal marker (Mizushima et al., 2010). The GABARAP subfamily proteins

function at the maturation stage (Feng et al., 2014). There are four orthologs of Atg4 in mammalian cells, in which Atg4B carries out the primary role in autophagy (Feng et al., 2014). In the Atg12 system, Atg12 is covalently conjugated to Atg5 through Atg7 and Atg10. The Atg12-Atg5 complex then interacts with Atg16. These two protein conjugation systems, which are highly conserved in higher eukaryotes, are critical for the elongation of autophagosomal membranes (Chen and Klionsky, 2011).

Post-translational regulation of the core autophagic machinery

Autophagy can be activated by multiple stress conditions. Amino acid starvation is a well-known and widely used stimulus to induce autophagy. Other known autophagy inducers include glucose starvation, mitochondrial stress, microbial infection, protein aggregation, exercise, and multiple drugs (He et al., 2012; Kroemer et al., 2010). Excessive amino acids and growth factors are suppressors of autophagy. The activation and suppression of autophagy are tightly regulated by multiple post-translational modifications of different autophagy proteins. These regulatory events act in coordination to help cells, tissues and organisms make correct decisions under different circumstances.

Post-translational modification of the Atg1 (Ulk1) complex

Multiple kinases are known to regulate autophagy by phosphorylating the Atg1 complex under different physiological conditions. In yeast, the target of rapamycin (TOR) is one of the best-characterized negative regulators of autophagy and it acts by phosphorylating the

Atg1 complex (Kroemer et al., 2010). TOR is activated when the energy and nutrient status of the cell is sufficient. It can also be activated by excessive amino acid and growth factors. When TOR is activated, it directly phosphorylates Atg1 and inhibits its kinase activity. TOR also phosphorylates Atg13 to reduce its affinity for Atg1, resulting in the inhibition of autophagy induction. When the cellular energy, amino acid or growth factor levels in the cell are low, the activity of TOR is inhibited to allow autophagy induction (Neufeld, 2010). In mammals, the ortholog of TOR is mechanistic target of rapamycin (mTOR). It forms two complexes mTORC1 and mTORC2. mTORC1 phosphorylates Ulk1 and ATG13 to inhibit autophagy (McEwan and Dikic, 2011). mTORC1 inhibitors such as rapamycin and torin1 are commonly used as autophagy inducers. Upon starvation or rapamycin/torin1 treatment, mTORC1 dissociates from Ulk1, which allows Ulk1 to phosphorylate FIP200 and facilitates autophagy induction (McEwan and Dikic, 2011).

In yeast, cAMP-activated protein kinase A (PKA) also phosphorylates Atg13 directly under nutrient-rich conditions and inhibits autophagy (Stephan et al., 2009). The PKA phosphorylation sites are different from the TORC1 sites. Phosphorylation of Atg13 by PKA is sufficient to inhibit autophagy by preventing the association of Atg13 and the PAS (McEwan and Dikic, 2011). However, to date, Atg13 has not been identified as a target of PKA in mammals and this regulatory mechanism may not be conserved (McEwan and Dikic, 2011).

In mammals, in response to stimuli such as starvation and hypoxia, AMPK, a central kinase in lipid and glucose metabolism is activated. Activated AMPK phosphorylates Tsc1/2, upstream regulatory proteins of mTOR and leads to mTORC1 inhibition (Inoki et al., 2012). Active AMPK also directly phosphorylates Ulk1 to promote the activation of autophagy (Kim et al., 2011). Snf1, the yeast ortholog of AMPK also positively regulates autophagy. However, the molecular mechanism by which Snf1 regulates autophagy remains elusive (Chen and Klionsky, 2011).

Acetylation is also an important post-translational modification that plays critical roles in autophagy. Acetylation had been shown to modulate the activity of the Ulk1 complex. In response to stimuli such as growth factor deprivation, TIP60 acetylates Ulk1 and facilitates autophagy induction (Lin et al., 2012). Acetylation can also regulate the functions of other Atg proteins, which will be discussed later in this chapter.

Post-translational modification of the class III PI3K complex

The class III PI3K complex is also a major target of post-translational modifications. AMPK suppresses overall PI3P production and protects cells from starvation by phosphorylating Vps34 (Kim et al., 2013). Under nutrient-rich conditions, Akt phosphorylates Beclin 1 on serine residues and facilitates the interaction between Beclin 1 and 14-3-3 and Vimentin, leading to autophagy inhibition (Wang et al., 2012). When activated, the epidermal growth factor receptor (EGFR) phosphorylates tyrosine residues of Beclin 1, which contributes to tumor progression in xenografts formed by non-small lung carcinoma cells (Wei et al., 2013).

In response to autophagy-inducing stimuli, Beclin 1 can be phosphorylated by DAPK, AMPK, and Ulk1 (Kim et al., 2013; Russell et al., 2013; Zalckvar et al., 2009). Phosphorylation of Beclin 1 by DAPK leads to the dissociation of Beclin 1 from Bcl-2 and upregulates autophagy (Zalckvar et al., 2009). In response to glucose starvation, AMPK phosphorylates Beclin 1 S93 and S96 to promote autophagy (Kim et al., 2013). Ulk1 phosphorylates Beclin 1 S14, which also leads to autophagy induction (Russell et al., 2013). Autophagy can also be regulated by phosphorylation of Bcl-2. In response to starvation, Bcl-2 is phosphorylated by JNK1 and dissociates from Beclin 1, which leads to autophagy induction (Wei et al., 2008).

Post-translational modifications of the two ubiquitin-like protein conjugation complexes

LC3 is directly phosphorylated by PKA, which regulates its function in autophagy (Cherra et al., 2010). Phosphorylation of LC3B by PKA inhibits its recruitment to autophagosomes (Cherra et al., 2010). LC3B can also be phosphorylated by PKC (McEwan and Dikic, 2011). Inducers of autophagy such as rapamycin cause dephosphorylation of LC3, and a nonphosphorylatable LC3 mutant exhibits enhanced puncta formation (Cherra et al., 2010).

Acetylation is also an important event in the regulation of the ubiquitin-like protein conjugation complexes. Under nutrient-rich condition, p300 acetyltransferase directly binds to Atg7 and acetylates Atg5, Atg7, LC3 and Atg12 (Lee and Finkel, 2009). Acetylation of these proteins by p300 inhibits autophagy. In response to starvation, the NAD-dependent deacetylase Sirt 1 interacts with Atg5, Atg7 and Atg8 and deacetylates these proteins, which

is essential for autophagy induction (Lee et al., 2008; Lee and Finkel, 2009). It is also reported that Esa1 (TIP60 in mammals) can acetylate Atg3, which promotes the Atg3-Atg8 interaction (Yi et al., 2012).

Regulation of autophagy by Bcl-2

The Bcl-2 family proteins such as Bcl-2, Mcl-1 and Bcl-XL are anti-apoptotic proteins. These proteins block autophagy by interacting with the BH3 domain of Beclin 1 and sequestering Beclin 1 away from the autophagy nucleation complex (Wang et al., 2013). The interaction between Bcl-2 and Beclin 1 occurs at the mitochondria and the ER, but only ER localized Bcl-2 can inhibit autophagy (Pattingre et al., 2005).

The interaction between Beclin 1 and Bcl-2 is regulated by protein binding partners and post-translational modifications. BNIP3 competes with Beclin 1 for interaction with Bcl-2 and HMGB1 competes with Bcl-2 for interaction with Beclin 1 (Bellot et al., 2009; Tang et al., 2010). These interactions lead to autophagy induction. For post-translational regulation, phosphorylation of Bcl-2 by JNK1 on T69, S70 and S84 in response to stimuli such as starvation leads to the dissociation of Beclin 1 and Bcl-2 (Wei et al., 2008). Mutating these three JNK1 phosphorylation sites to alanine abolishes starvation and exercise-induced autophagy (He et al., 2012; Wei et al., 2008). In contrast, DAPK can phosphorylate the BH3 domain of Beclin 1, leading to dissociation of Bcl-2/Beclin 1 and autophagy induction (Zalckvar et al., 2009).

Autophagy and cancer

Autophagy is critical for regulating the pathogenesis of multiple diseases such as neurondegeneration, myodegenerative diseases, liver diseases, cardiac diseases, infectious diseases, inflammation and cancer (Levine and Kroemer, 2008).

Autophagy plays dual roles in cancer. On one hand, autophagy can prevent tumorigenesis by removing damaged protein and organelles, thereby reducing cellular genotoxic stress. The first study showing that autophagy is critical for tumor suppression comes from the study of monoallelic loss of *Becn1* in mice (Qu et al., 2003; Yue et al., 2003); these mice have an increased incidence of spontaneous tumors, including lung adenocarcinoma, hepatocellular carcinoma, lymphoma, and mammary gland neoplastic lesions (Qu et al., 2003). In humans, monoallelic loss of *BECN1* was found in 40-75% breast, prostate, and ovarian cancer patients, suggesting that autophagy deficiency may contribute to the development of human cancers (Liang et al., 1999). On the other hand, autophagy can promote tumor growth and survival by providing nutrients to the fast-growing tumors under unfavorable conditions. Increased autophagy is seen in tumor cells under hypoxia (Mazure and Pouyssegur, 2010). Moreover, in some studies, autophagy inhibitors significantly increase tumor cell death when used together with chemotherapy (Cloonan and Williams, 2011; Stein et al., 2010).

II. Introduction to the kinases investigated in this study

MK2 and MK3

MAPKAPK2/3 (MK2/3) are MAPK-activated protein kinases, which are activated by the p38 module in response to multiple stress conditions including LPS treatment, UV radiation, cytokine treatment, heat shock and osmotic stress (Ronkina et al., 2008). While there are no known diseases associated with MK2, MK3 is commonly deleted in small cell lung cancer (Sithanandam et al., 1996). MK2 knockout mice are resistant to endotoxic shock and MK2/3 double-knockout accentuates the phenotype (Ronkina et al., 2007). MK2 and MK3 share high sequence identity (75%) (Ronkina et al., 2008). They contain an N-terminal domain, a kinase domain, a functional nuclear localization signal (NLS) and nuclear export signal (NES) (Gaestel, 2006). The N-terminal domain of MK2 and MK3 interacts with SH3 domains. The NLS encompasses a docking domain (D domain) through which MK2/3 interact with p38α/β. The activation of MK2/3 depends on the kinase activity of p38. In response to stimuli that activate p38, p38 phosphorylates MK2 on T222 and MK3 on T201 within the activation loop (**Fig. 1. 2**). The phosphorylation of T334 in MK2 and T313 in MK3, which is also mediated by p38, leads to the nuclear export of MK2/3 (**Fig. 1. 2**) (Gaestel, 2006). In quiescent cells, MK2/3 predominantly localize to the nucleus, whereas in response to stimulation, they are rapidly activated by T334/313 phosphorylation and traffic to the cytoplasm (Gaestel, 2006).

MK2/3 are ubiquitously expressed in different organs and tissues (Gaestel, 2006). Expression levels are highest in the heart, skeletal muscle and the kidney (Cargnello and Roux, 2011). MK2 and MK3 share the same sets of substrates (Clifton et al., 1996). Although the kinase

activities of MK2 and MK3 are comparable *in vitro*, the kinase activity of MK2 is higher than MK3 *in vivo* (Ronkina et al., 2007).

Multiple substrates of MK2 and MK3 have been identified. They function in actin remodeling and cell migration, cell cycle control, cytokine production and transcriptional regulation (Cargnello and Roux, 2011). Hsp25 and Hsp27 are among the first identified substrates of MK2 and MK3 (Sithanandam et al., 1996; Stokoe et al., 1992). The phosphorylation of Hsp25/Hsp27 has been used to detect the activation of MK2/3.

MK5

MK5 shares 38% sequence homology with MK2 (Clifton et al., 1996). Its kinase activity depends on the phosphorylation of T182 (New et al., 1998). Although p38 phosphorylates T182 *in vitro*, stimuli such as osmotic stress and LPS treatment that strongly activate p38 *in vivo* fail to activate MK5. It is reported that MK5 is activated by ERK3 and ERK4 (Clifton et al., 1996).

III. Figures

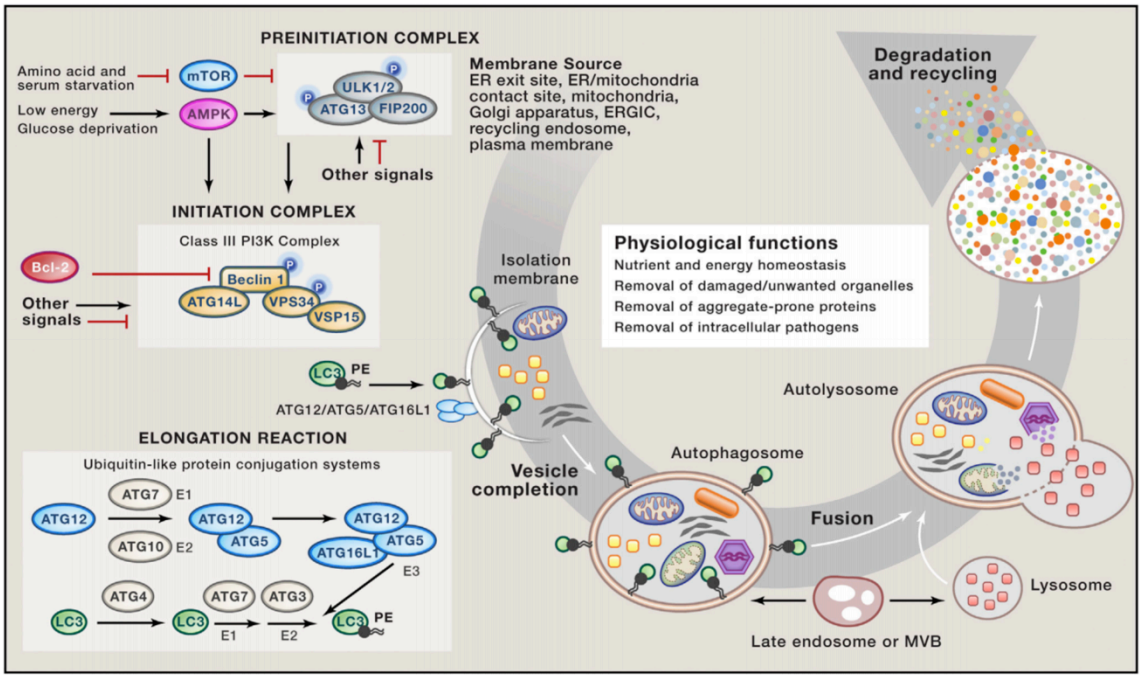

Figure 1. 1. Overview of the autophagy pathway.

Autophagy is initiated by the Ulk1 complex, which consists of Ulk1/2, Atg13 and FIP200. The Ulk1 complex is regulated by mTOR and AMPK. When autophagy is initiated, the class III PI3K complex forms. Bcl-2 inhibits autophagy by interacting with Beclin 1 in this complex. Autophagy also requires Atg12 and LC3 ubiquitin-like protein conjugation systems. The membrane sources of autophagosomes and the physiological functions of autophagy are also indicated in this figure. Adapted with permission from (Green and Levine, 2014).

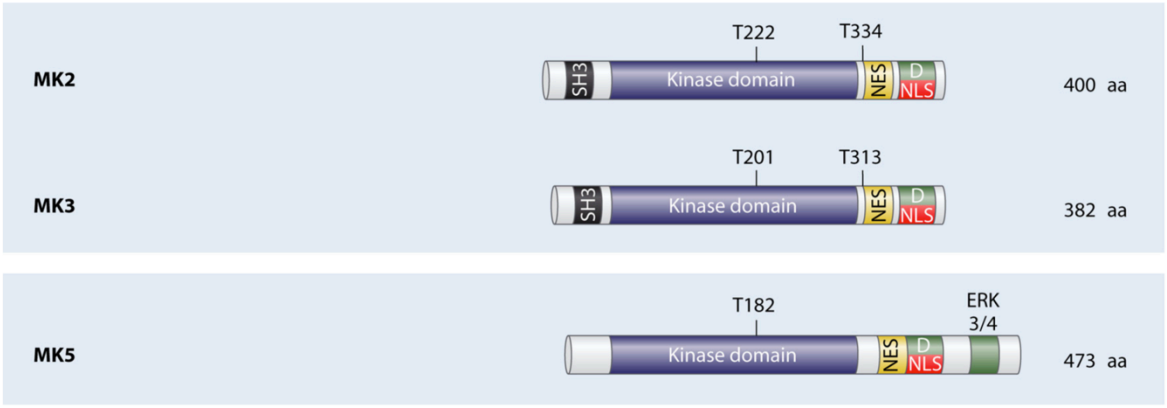

Figure 1. 2. Schematic representation of the structure and activation of MK2, MK3 and MK5.

MK2, MK3 and MK5 all contain a kinase domain, a functional NES and NLS. Activation of these kinases requires phosphorylation of a serine residue in the kinase domain. Phosphorylation of T334 in MK2 and T313 in MK3 promotes nuclear export of these kinases Adapted from (Clifton et al., 1996).

CHAPTER TWO

Materials and Methods

I. Methods for Yeast Experiments

Yeast strains and culture conditions

S. cerevisiae strains used in this study are listed in Table 1. Unless noted otherwise, yeasts were grown in YPD (20 g/L peptone, 10 g/L yeast extract and 20 g/L glucose). For nitrogen starvation, yeasts were grown in SD-N (1.7 g/L yeast nitrogen base without amino acids and ammonium sulfate and 20 g/L glucose). Solid medium contained 20 g/L agar.

Budding assay

$5x10^5$ cells/ml were grown in 5 ml fresh YPD for 4 h to early midlog phase (OD_{600} 0.2-0.3). Samples were washed 3 times with SD-N and 1/3 of the culture (labeled "YPD") was fixed in 70% ethanol for 2 h and washed with 50 mM sodium citrate, pH 7.4. After brief sonication, cells with or without buds were quantified using DIC microscopy. The remainder of the culture was starved in SD-N for 4 h or 24 h. Samples were then processed and analyzed as described for the YPD samples.

Quantification of yeast cell numbers

Yeast cells were washed 3 times in autoclaved H_2O prior to resuspension in either YPD or SD-N. Cell numbers were determined by using a hemocytometer (Hausser Scientific) according to the manufacturer's instructions.

Yeast transformation

Yeasts were transformed with a plasmid encoding HA-Snf1(McCartney and Schmidt, 2001) using the Frozen-EZ Yeast Transformation II Kit (Zymo Research) according to the manufacturer's instructions.

Flow cytometry

$5x10^5$ cells/ml were grown in 5 ml fresh YPD for 4 h to early midlog phase (OD_{600} 0.2-0.3). Samples were washed 3 times with SD-N and 1 ml of the culture was removed and fixed with 70% ethanol at 4 °C overnight. The remainder of the culture was starved in SD-N for 4 h before fixation with 70% ethanol. After overnight fixation, cells were washed twice with 50 mM sodium citrate, pH 7.4, incubated for 2 h at 37 °C with 0.25 mg/ml RNase A (Sigma,), washed twice with 50 mM sodium citrate, pH 7.4, and stained with 5 μg/ml propidium iodide (Roche) for 30 min in the dark. Cell cycle analysis was performed on a FACSCalibur (BD Biosciences) in the UT Southwestern Flow Cytometry Core Facility and the data were analyzed using FlowJo 8.8.6.

Cell survival assay

Yeast strains were grown in YPD or SD-N for 4 h and tested for survival by plating 100 cells at 30°C for 48 h on YPD plates. Cell survival percentage was calculated as the number of colonies divided by the total number of plated cells.

Heat shock assay

Yeasts were incubated in a 50°C water bath for 0 or 15 min and chilled on ice for 2 min. Yeasts were then plated on YPD plates and grown at 30°C for 48 h. Colony numbers were quantified.

Glycogen and trehalose assay

Glycogen and trehalose were hydrolyzed to glucose as previously described (Parrou and Francois, 1997). 2 x 10^8 cells were harvested. Glucose levels were determined using the Glucose (GO) Assay Kit (Sigma, GAGO20). OD_{540} was measured using a POLARstar Omega multi-mode microplate reader (BMG Labtech).

Protein extraction and western blotting

Protein was extracted from yeast cells grown in YPD or SD-N. 2 x 10^8 cells were harvested from each sample. Yeasts were lysed in 500 µl RIPA buffer (50 mM Tris, pH 8.0, 150 mM NaCl, 0.1% SDS, 1% NP40 substitute IGEPAL CA-630 (Sigma, I8896), 0.5% sodium

deoxycholate (Sigma) containing the complete protease inhibitor cocktail (Roche) and the halt phosphatase inhibitor cocktail (Thermo Scientific). HA-Snf1 was immunoprecipitated using anti-HA agarose conjugate (Santa Cruz). Proteins were resolved using 4-15% TGX gels (Bio-Rad) and transferred to PVDF membranes. HA-Snf1 was detected with an HA-specific HRP-conjugated mouse monoclonal antibody (Santa Cruz). Phospho-Snf1 was detected with a phospho-AMPK alpha (Thr172) rabbit monoclonal antibody (Cell Signaling Technology).

Immunofluorescence

Yeast cells were grown to early midlog phase (OD_{600} ~0.2-0.3), washed 3 times with SD-N and starved in SD-N for 4 h. Cells were then fixed with 4% paraformaldehyde for 45 min at 30 °C, washed once with 100 mM potassium phosphate, pH 6.5, and washed twice with P solution (100 mM potassium phosphate, pH 6.5, 1.2 M sorbitol). 15 μL zymolase (100T; Zymo Research) and 2.5 μL β-mercaptoethanol were added to 500 μL cells in P solution. After 1 h incubation at 30 °C, cells were washed twice with P solution and placed on poly-D-lysine-coated chamber slides (Electron Microscopy Sciences) for 10 min. Cells were washed with phosphate-buffered saline (Sigma) containing 5 mg/ml BSA (Sigma) (PBS-BSA). Anti-Tub1 antibody (Novus Biologicals) was added at a dilution of 1:100 in PBS-BSA, and slides were incubated overnight at 4 °C. The slides were washed 3 times with PBS-BSA and secondary antibody (Alexa 594; Invitrogen) was added at a dilution of 1:2,000 in PBS-BSA and incubated in the dark for 2 h. Cells were washed 3 times with PBS-BSA, mounted with

DAPI-mounting medium (Vector Laboratories) and sealed with nail polish. Images were captured using a Zeiss Axioplan 2 fluorescence microscope.

Live cell imaging

Yeasts were washed three times with SD-N, grown on 1% (w/v) agarose pads in SD-N and monitored under a DIC microscope. Pictures were taken at the indicated time points.

II. Methods for Mammalian Experiments

Cell culture

HeLa, HEK293T, MEF cells (transformed) and MCF-7 cells were grown in DMEM supplemented with 10% FBS, 100 U/ml penicillin and 100 μg/ml streptomycin. Beclin 1 shRNA U2OS cells were grown in DMEM supplemented with 10% Tet-free FBS. HeLa-Neo, HeLa-Bcl-2, HeLa-Bcl-2 AAA, HeLa-GFP-LC3 and SKNSH-Flag-Beclin 1 cells were grown in DMEM supplemented with 10% FBS and 0.1g/L G418. MCF-7 cells stably expressing Beclin 1 (or Beclin S90 mutants) were grown in DMEM supplemented with 10% FBS, 0.01mg/ml human recombinant insulin and 1μg/ml puromycin. MK2/3 double-knockout cells stably expressing Beclin 1 (or Beclin 1 S90 mutants) were grown in DMEM supplemented with 10% FBS and 1μg/ml puromycin. Primary Bcl-2 AAA MEF cells were grown in DMEM supplemented with 10% heat inactivated FBS, 1xMEM nonessential amino acids, 2mM L-glutamine, 20mM HEPES, pH 7.3, 0.1mM β-mercaptoethanol, 100 U/ml

penicillin and 100 μg/ml streptomycin. All cells were maintained at 37°C in humidified, concentrated CO_2 (5%) atmosphere.

Plasmids

The human *beclin 1* gene was inserted into the EcoRI/BmHI restriction site of the pBICEP-CMV2 vector. pBICEP-CMV2-Beclin 1 S90 mutants and pBABE-puro-Beclin 1 S90 mutants were constructed using a QuickChange site mutagenesis kit (Agilent technologies). The shRNA non-targetable Beclin 1 plasmids were constructed using PCR and ligation. All of the constructs were confirmed by sequencing.

Antibodies

Flag was detected using an anti-Flag M2 HRP antibody (1:2000) (Sigma-Aldrich). The phospho-specific Beclin 1 S90 antibody was produced by PhosphoSolutions and used at a concentration of 1:500. Beclin 1, Hsp27, p-Hsp27, Actin, MK2, p62 and LC3 were detected using a rabbit or goat anti-Beclin 1 antibody (1:1000), a rabbit anti-Hsp27 antibody (1:200), a rabbit anti-p-Hsp27 antibody (1:200), an anti-β-Actin HRP antibody (1:2000) (Santa Cruz Biotech Inc.), a rabbit anti-MK2 antibody (1:1000) (Cell Signaling Technology), a mouse anti-p62 antibody (1:2000) (Abnova) and a rabbit anti-LC3 antibody (1:1000) (Novus Biologicals).

Transient transfection

Lipofectamine 2000 (Life Technologies) was used for cell transfection according to the manufacturer's protocol. For the GFP-LC3 assay, GFP-LC3 and Beclin 1 (or Beclin 1 S90 mutants) were co-transfected at a molecular ratio of 1:2. For the western blotting in Beclin 1 shRNA U2OS cells, shRNA non-targetable Beclin 1 (or Beclin 1 S90 mutants) and MK2 mutants were co-transfected at a molecular ratio of 1:1.

Protein extraction and immunoblotting

Cells were lysed in lysis buffer (100mM Tris, pH 8.0, 150 mM NaCl, 1mM EDTA, 1% Triton X-100) with protease (Roche) and phosphatase inhibitors cocktail (Pierce) for 30 min. Cell lysates were separated on 4-15% TGX gels (Bio-Rad laboratories), transferred to PVDF membranes (Bio-Rad laboratories), and probed with the indicated antibodies.

Radioactive isotope labeling

HeLa cells were plated on 6 cm dishes. The next day, cells were transfected with pBICEP-CMV2, pBICEP-CMV2-Beclin 1, or pBICEP-CMV2-Beclin 1 S90A using lipofectamine 2000. On the second day after transfection, cells were grown in phosphate-free medium (phosphate free DMEM + 10% FBS) for 3 h. The cells were then washed with phosphate-free EBSS 3 times and were grown in phosphate-free EBSS or phosphate-free normal medium supplemented with 40 μCi p-33 for 2 h. The cells were washed three times with PBS, and lysed with lysis buffer (100mM Tris, pH 8.0, 150 mM NaCl, 1mM EDTA, 1%

Triton X-100 with protease and phosphatase inhibitors) for 30 min. The lysate was centrifuged for 10 min at 13,000 rpm at 4°C. The supernatants were collected and adjusted to equal protein concentrations using the Bradford assay. Nine μL α-Flag agarose (sigma, M2) was added to each sample and samples were rotated at 4°C overnight. The agarose was washed 3 times with PBS. Thirty μL SDS loading buffer was added and the samples were boiled at 95°C for 5 min. Ten μL of each sample were loaded on 4-15% TGX gels (Biorad).

Peptide synthesis and kinase screen

Peptides based on amino acid sequences of human Beclin 1 were synthesized (JPT Peptide Technologies) and used as substrates for an *in vitro* protein kinase screen. The peptides were dissolved in 50 mM HEPES, pH 7.5 at a concentration of 200 μM. A radiometric Streptavidin-FlashPlate^{TM}-based protein kinase assay was performed for measuring the kinase activity of 190 serine/threonine kinases (ProQinase).

Immunoprecipitation

To immunoprecipitate endogenous Beclin 1, immunoprecipitation was performed using a polyclonal goat anti-Beclin 1 antibody (1:50) (Santa Cruz Biotech Inc.). To immunoprecipitate Flag-tagged Beclin 1, immunoprecipitation was performed using a monoclonal anti-Flag M2 antibody pre-conjugated to agarose (1:20) (Sigma-Aldrich).

Metabolic labeling

Transfected HeLa cells were grown in phosphate-free medium (phosphate free DMEM + 10% dialyzed FBS) for at least 3 h. The cells were washed with phosphate-free HBSS and grown in phosphate-free HBSS or phosphate-free medium supplemented with 40μCi/ml ^{33}P-orthophosphate for 2 h. The cells were washed with PBS, and lysed in lysis buffer (100 mM Tris, pH 8.0, 150 mM NaCl, 1mM EDTA, 1% Triton X-100) with protease (Roche) and phosphatase inhibitors cocktail (Pierce) for 30 min. Flag-Beclin 1 was immunoprecipitated with an anti-Flag M2 agraose (Sigma-Aldrich), separated in 4-15% TGX gels (Bio-rad Laboratories) and visualized by autoradiography.

Soft agar assay

A soft agar assay using MCF-7 cells stably expressing Beclin 1 (and Beclin 1 S90 mutants) was performed as described previously (Wang et al., 2012).

Xenograft assay

A 1.7 mg estrogen pellet (60-day release time) (Innovative Research of America) was injected in the neck region of 7-week old female *nu/nu* mice. After one week, 5x10^6 MCF-7 cells stably expressing Beclin 1 (or Beclin 1 S90 mutants) were injected into the upper right mammary fat pad of each mouse. Tumor width and length were measured twice a week for a total experiment duration of 8 weeks. Each group contained 11 mice.

In vitro kinase assay

pBICEP-CMV2 Beclin 1 or pBICEP-CMV2 Beclin 1 S90A was transfected to HEK293 cells using lipofectamine 2000 (Invitrogen) (6 μg DNA was transfected to each 10 cm dish). After 24 h, each dish of cells was lysed with 500 μL lysis buffer (100 mM Tris pH 8.0, 150 mM NaCl, 1mM EDTA, 1% Triton X-100 with protease inhibitors) for 30 min at 4°C. Flag-Beclin 1 was immunoprecipitated by 75 μL Flag-agarose (M2, sigma) for 3 h at 4°C. The beads were washed twice with lysis buffer and another 2 times with phosphatase buffer. The samples were then treated with λ-protein phosphatase (Biolabs) according to the manufacturer's protocol. For 60 μL Flag agarose, 4 μL λ-protein phosphatase was used. The agarose was washed twice with lysis buffer with phosphatase inhibitors, and another 2 times with kinase buffer (60 mM HEPES, pH 7.6, 3 mM $MgCl_2$, 3 mM $MnCl_2$, 3 mM Na_3VO_4, 1.2mM DTT). For each *in vitro* kinase reaction, 15 μL Flag agarose was mixed with 15 μL kinase buffer (with 1 μM ATP). The kinases were added to a final concentration of 0.16 μM. The reactions were incubated at 30°C for 30 min. Thirty μL SDS loading buffer was added to each reaction and the samples were incubated at 95°C for 2 min. After brief centrifugation, the supernatants were loaded onto 4-15% precasted TGX gels (Biorad), transferred to PVDF membranes and incubated with the indicated antibodies.

Immunohistochemistry

Mouse tissues were fixed in 4% PFA, embedded in paraffin, cut to approximately 5 microns and affixed onto glass slides. Before staining, the slides were deparaffinized. The slides were

washed twice with xylene and then incubated in xylene-ethanol (1:1 v:v) for 3 min. The slides were then washed with ethanol twice and rehydrated by successive incubations in 95%, 70% and 50% ethanol for 3 min each. The slides were rinsed in water and placed in a microwavable container with the antigen retrieval buffer (10 mM sodium citrate, 0.05% Tween 20 pH 6.0) and boiled in the microwave for 15 min. The slides were then rinsed in water for 10 min and washed twice with TBS with 0.05% Tween 20 for 5 min each time. The slides were blocked with 5% BSA-TBST for 1 h and incubated in primary antibody (1:50 or 1:100 dilution in 5% BSA-TBST) at 4°C overnight. The slides were washed twice with TBST, incubated in 0.3% H_2O_2 in TBS for 15 min and then incubated with HRP-conjugated secondary antibody (1:1500 dilution in 5% BSA-TBST) for 1 h at room temperature. The slides were washed 3 times with TBS and developed with DAB for 10 min at room temperature. After washing with water, the slides were dehydrated and mounted for microscopy analysis.

Immunofluorescence

Slide preparation was done in the same way as mentioned in the immunohistochemistry section. After antigen retrieval, the slides were treated with 0.2% Triton X-100 in PBS for 45 min at room temperature. The slides were then washed 3 times with PBS, blocked with 5% BSA in PBS and incubated with the indicated primary antibodies (1:50 in PBS-BSA) at 4°C overnight. The slides were washed 3 times with PBS and incubated with secondary antibodies (1:2000 in PBS-BSA) for 1 h at room temperature. After washing 3 times with

PBS, the slides were mounted with DAPI-containing mounting medium and sealed with nail polish.

Mouse Starvation and Tissue Preparation

8-week-old C57BL/6 mice and Bcl-2 AAA knock-in mice in a C57BL/6 background were starved for 48 h and thigh muscles were snap-frozen in liquid nitrogen. The thigh muscles were homogenized and protein was extracted in lysis buffer (100mM Tris, pH 8.0, 150 mM NaCl, 1mM EDTA, 1% Triton X-100) with protease (Roche) and phosphatase inhibitors cocktail (Pierce)).

Table 2. 1. Yeast strains used in this study.

Strain	Genotype	Reference
AHY001	SEY6210 *atg11*Δ:: HIS5	(Kim et al., 2001b)
JCY3000	SEY6210 *atg6* Δ *::HIS3*	(Robinson et al., 1988)
MGY101	SEY6210 *atg5* Δ *::LEU2*	(Shintani et al., 2002)
SEY6210	*MATα leu2-3, 112 ura3-52 hisΔ200 trp1-Δ901 lys2-801 suc2-Δ9*	(George et al., 2000)
TKYM139	SEY6210 *atg32* Δ *::LEU2*	(Kanki et al., 2009)
TVY1	SEY6210 *pep4* Δ::LEU2	(Gerhardt et al., 1998)
VDY101	SEY6210 *atg7* Δ *::LEU2*	(Seaman et al., 1997)
WHY001	SEY6210 *atg1* Δ *::HIS5*	(Kim et al., 1999)
WPHYD7	SEY6210 *atg8* Δ *::LEU2*	(Kim et al., 2001a)
ZFY6	SEY6210 *atg22* Δ *::TRP1*	(Yang et al., 2006)
ZFY22	SEY6210 *avt3Δ::HIS3 avt4Δ::URA3 atg22Δ::TRP1*	(Yang et al., 2006)

CHAPTER THREE

Autophagy is required for G_1/G_0 quiescence in response tonitrogen starvation in *Saccharomyces cerevisiae*

I. Abstract

In response to starvation, cells undergo increased levels of autophagy and cell cycle arrest but the role of autophagy in starvation-induced cell cycle arrest is not fully understood. Here we show that autophagy genes regulate cell cycle arrest in the budding yeast *Saccharomyces cerevisiae* during nitrogen starvation. While exponentially growing wild-type yeasts preferentially arrest in G_1/G_0 in response to starvation, yeasts carrying null mutations in autophagy genes show a significantly higher percentage of cells in G_2/M. In these autophagy-deficient yeast strains, starvation elicits physiological properties associated with quiescence, such as Snf1 activation, glycogen and trehalose accumulation, as well as heat shock resistance. However, while nutrient-starved wild-type yeasts finish the G_2/M transition and arrest in G_1/G_0, autophagy-deficient yeasts arrest in telophase. Our results suggest that autophagy is crucial for mitotic exit during starvation and appropriate entry into a G_1/G_0 quiescent state.

II. Introduction

Eukaryotic cell growth and proliferation are regulated by nutrients, and the budding yeast, *Saccharomyces cerevisiae,* provides an excellent model for studying such regulation. In response to nutrient deprivation, cells stop proliferating, undergo cell cycle arrest, and enter a reversible state of quiescence, usually in G_0 of the cell cycle (Jorgensen and Tyers, 2004). It is commonly accepted that the decision to proliferate is made when cells are in G_1, which is

called Start in budding yeast. This decision is regulated by a variety of nutrient-sensing kinases including Snf1, PKA, Tor1 and Tor2, Sch9 and Pho85-Pho80 (Smets et al., 2010). Once yeast cells have passed Start, they usually traverse all phases of the cell cycle until reaching Start again. If a decision is made not to proliferate, haploid cells preferentially arrest at Start and enter quiescence with a 1N DNA content.

Yeasts can also enter quiescence – at least during carbon starvation – through other cell cycle phases besides G_0/G_1, although the ability to give rise to progeny is diminished (Daignan-Fornier and Sagot, 2011; Laporte et al., 2011; Wei et al., 1993). In cells that have entered quiescence upon carbon source exhaustion, quiescence exit can be triggered by glucose addition. These observations have given rise to the notion that quiescence entry and exit may be governed primarily by cellular metabolic status and are not invariably coupled to the cell cycle. Nonetheless, the cellular pathways that govern the stage of the cell cycle at which yeast enter quiescence during starvation remain poorly understood.

Autophagy is a highly conserved pathway in which cytoplasmic contents are degraded and recycled in response to stressors including starvation. Autophagy is critical for maintaining cellular energy homeostasis and regulating cell growth (Levine and Kroemer, 2008). The core yeast autophagy machinery can be divided into 4 major subgroups (Yang and Klionsky, 2010). The Atg1-Atg13-Atg17 serine/threonine kinase complex is crucial for the initiation step of autophagy. The Vps30/Atg6, Vps15, Vps34, and Atg14 lipid kinase complex is essential for the formation of the phagophore. The vesicle elongation step of autophagy includes 2 ubiquitin-like protein systems; the core members are Atg8, Atg12, Atg7, Atg10, Atg3, Atg4, Atg16 and Atg5. In addition, the Atg9 cycling system functions in autophagosome formation.

Previous studies showed that some autophagy genes participate in cell cycle regulation. For example, mice lacking *Becn1*, the mammalian ortholog of yeast *VPS30/ATG6*, have abnormal cell proliferation in mammary epithelial ducts and splenic germinal center lymphocytes (Qu et al., 2003); mice lacking *Ambra1* have increased cell proliferation in fetal brain (Fimia et al., 2007); and *atg7*$^{-/-}$ mouse embryonic fibroblast cells have impaired TRP53/p53-mediated cell cycle arrest (Lee et al., 2012). In the budding yeast, *Saccharomyces cerevisiae*, autophagy and G_1/G_0 cell cycle arrest are both induced after switching the cells from a nutrient-rich environment to nutrient-limited conditions (Abeliovich and Klionsky, 2001; Gray et al., 2004). However, it is not clear whether autophagy regulates G_1/G_0 cell cycle arrest.

In this study, we used the budding yeast *Saccharomyces cerevisiae* as a model system to study the role of autophagy in cell cycle regulation. Similar to mammalian cells, which arrest in G_1/G_0 after serum starvation (Zetterberg and Larsson, 1985), the majority of wild-type yeasts arrest in G_1/G_0 after nitrogen starvation (Gray et al., 2004). In contrast, we found that the majority of autophagy-deficient yeasts arrest in telophase after nitrogen starvation and, interestingly, still exhibit quiescence-specific phenotypes. Based on these results, we conclude that autophagy genes are required for yeast to traverse the cell cycle and properly arrest in G_1/G_0 in response to starvation.

III. Results

Autophagy-deficient yeasts fail to enter G_1/G_0 in response to starvation

To investigate the role of autophagy in cell cycle regulation during starvation, we examined whether yeasts with null mutations in different essential autophagy genes (*ATG1*, *ATG5*,

VPS30/*ATG6*, *ATG7*, and *ATG8*) arrest in G_1/G_0 after nitrogen starvation. During growth in YPD medium, about 30% of both wild-type and *atg1*Δ, *atg5*Δ, *vps30*Δ/*atg6*Δ, *atg7*Δ and *atg8*Δ yeast cells were in G_1/G_0, as quantified by the percentage of cells without buds. After starving exponentially growing yeasts in nitrogen starvation medium (SD-N) for 4 h, greater than 80% of wild-type yeasts entered G_1/G_0 (**Fig. 3. 1**). In contrast, the percentage of *atg1*Δ, *atg5*Δ, *vps30*Δ/*atg6*Δ, *atg7*Δ and *atg8*Δ yeasts in G_1/G_0 only minimally increased in response to nitrogen starvation. The magnitude of this increase was markedly less than in wild-type yeasts indicating that autophagy-deficient yeasts have a defect in G_1/G_0 arrest in response to nitrogen starvation. This defect in G_1/G_0 arrest in autophagy-deficient yeast strains persisted at 24 h after nitrogen starvation (**Fig. 3. 2**).

To gain further insight into the mechanism by which autophagy functions in permitting yeast cells to arrest in G_1/G_0 in response to nitrogen starvation, we examined the phenotypes of yeast strains containing null mutations in genes encoding vacuolar permeases (*atg22*Δ and *atg22*Δ *avt3*Δ *avt4*Δ) (Yang et al., 2006), in selective autophagy genes (*atg11*Δ and *atg32*Δ) (Kanki et al., 2009; Kim et al., 2001b) and in a vacuolar protease gene (*pep4*Δ) (Gerhardt et al., 1998). *atg22*Δ, *atg22*Δ *avt3*Δ *avt4*Δ, *atg11*Δ and *atg32*Δ mutant yeasts did not significantly differ from wild-type yeasts with respect to the percentage of cells in G_1/G_0 after nitrogen starvation (**Fig. 3. 1, Fig. 3. 2**). In contrast, *pep4*Δ yeasts, which are deficient in the maturation of vacuolar enzymes, showed a similar percentage of cells without buds in response to nitrogen starvation as *atg1*Δ, *atg5*Δ, *vps30*Δ/*atg6*Δ, *atg7*Δ and *atg8*Δ yeasts (**Fig. 3. 1, Fig. 3. 2**). Taken together, these observations suggest that the failure of *atg1*Δ, *atg5*Δ, *vps30*Δ/*atg6*Δ, *atg7*Δ and *atg8*Δ yeasts to arrest in G_1/G_0 in response to nitrogen starvation is not likely due to a deficiency in nutrient recycling or selective autophagy, but rather, may be due to defects in autophagic cargo degradation in the yeast vacuole.

To further confirm that autophagy-deficient yeasts fail to enter G_1/G_0 after nitrogen starvation, we measured DNA content using flow cytometry. Consistent with the budding assay data (**Fig. 3. 1**), the majority of wild-type, *atg22*Δ, *atg22*Δ *avt3*Δ *avt4*Δ, *atg11*Δ and *atg32*Δ cells had a 1N DNA content 4 h after nitrogen starvation. In contrast, the majority of *atg1*Δ, *atg5*Δ, *vps30*Δ/*atg6*Δ, *atg7*Δ, *atg8*Δ and *pep4*Δ yeasts had a 2N DNA content after starvation, indicating they were not in G_1/G_0 (**Fig. 3. 3, Fig. 3. 4**). Thus, both the budding assay and DNA content measurements indicated that yeast defective in general starvation-induced autophagy or vacuolar protease activity (but not in selective autophagy or vacuolar permease-dependent nutrient recycling) fail to properly arrest in G_1/G_0 following nitrogen starvation. Similar results were observed in response to glucose starvation (**Fig. 3. 5**)

Autophagy-deficient yeasts fail to progress through G_2/M in response to starvation

Next we examined whether autophagy-deficient yeasts continued to actively divide after nitrogen starvation. We measured the growth curve of wild-type and *vps30*Δ/*atg6*Δ yeast strains in both nutrient-rich YPD medium and in SD-N starvation medium (**Fig. 3. 6A and 3. 6B**). In YPD medium, wild-type and *vps30*Δ/*atg6*Δ yeasts grew at a similar rate (**Fig. 3. 6A**). In nitrogen starvation conditions, the growth of wild-type yeasts did not cease until after 4 h whereas, in contrast, autophagy-deficient yeasts stopped dividing almost immediately (**Fig. 3. 6B**). To exclude the possibility that the decreased numbers of *vps30*Δ/*atg6*Δ yeasts reflected increased cell death, we measured colony formation in wild-type and *vps30*Δ/*atg6*Δ yeasts after 4 h nitrogen starvation and found no difference in cell survival (**Fig. 3. 7**).

The accumulation of autophagy-deficient yeasts in G_2/M (rather than G_1/G_0) coupled with their failure to divide after nitrogen starvation raised the possibility that they have a defect in cell cycle progression through G_2/M. To examine this, we performed live cell imaging of wild-type and autophagy-deficient yeasts. Following nitrogen starvation, we found that the buds of wild-type yeast grew larger and eventually finished cytokinesis before the yeast cells became dormant. In contrast, the buds of autophagy-deficient *vps30*Δ/*atg6*Δ and *atg7*Δ yeasts stayed attached to the mother cells and failed to grow larger (**Fig. 3. 8**). Thus, autophagy may be necessary for proper transit through G_2/M after nitrogen starvation.

To further clarify the stage of G_2/M arrest in autophagy-deficient yeasts in response to nitrogen starvation, we stained DNA with DAPI and examined the morphology of the yeast spindle microtubules by immunofluorescence staining with an antibody recognizing the yeast tubulin, Tub1. We examined cells at 4 h after nitrogen starvation, a time point when the majority of wild-type yeasts lacked buds and were in G_1/G_0. In *atg6*Δ, *atg7*Δ and *pep4*Δ yeasts, nearly 100% of the cells arrested with buds had complete spindle disassembly and separation of the mother and daughter chromosomes, signifying an arrest in telophase with a failure to undergo cytokinesis (**Fig. 3. 9A and 3. 9B**). Thus, genes essential for autophagy and for vacuolar protease activity are required for mitotic exit during nitrogen starvation.

Autophagy-deficient yeasts have quiescence-specific phenotypes after nitrogen starvation.

Previous studies have shown that cell cycle mutants arrested in G_2/M can acquire characteristics of quiescence (Daignan-Fornier and Sagot, 2011). We investigated whether autophagy-deficient yeasts, although they fail to properly enter G_1/G_0 in response to nitrogen starvation, also display features of quiescence. First, we asked whether the yeast ortholog of

mammalian AMP-activated protein kinase (AMPK), Snf1, a crucial regulator of quiescence entry (Gray et al., 2004) is activated normally during nitrogen starvation in autophagy-deficient yeast strains. We found that Snf1 was phosphorylated within 30 min after nitrogen starvation in wild-type, *vps30*Δ/*atg6*Δ and *atg7*Δ yeasts (**Fig. 3. 10A**). Thus, Snf1 activation can occur in the absence of G_1/G_0 entry, and defects in Snf1 activation are unlikely to explain the failure of autophagy-deficient yeast to properly arrest in G_1/G_0 in response to nitrogen starvation.

Some of the phenotypic properties that characterize quiescence in yeast are metabolic changes, such as increased trehalose and glycogen accumulation and resistance to heat shock (Gray et al., 2004; Smets et al., 2010). In response to nitrogen starvation, wild-type, *vps30*Δ/*atg6*Δ, and *atg7*Δ yeasts accumulated trehalose and glycogen (**Fig. 3. 10B and 3. 10C**). In addition, all three strains showed starvation-induced heat resistance (**Fig. 3. 10D**). During exponential growth in YPD medium, the viability of wild-type, *vps30*Δ/*atg6*Δ, and *atg7*Δ strains was reduced after exposure to 50ºC for 20 min. Consistent with the known pro-survival function of autophagy in response to environmental stress, *vps30*Δ/*atg6*Δ and *atg7*Δ yeasts were more sensitive than wild-type yeasts to heat shock when grown in YPD. However, after 4 h of nitrogen starvation, *vps30*Δ/*atg6*Δ and *atg7*Δ yeasts were as heat-resistant as wild-type yeasts (**Fig. 3. 10D**). The same results were also observed for other autophagy-deficient yeast strains, including *atg1*Δ, *atg5*Δ, and *atg8*Δ (**Fig. 3. 10E**). Together, these results suggest that autophagy-deficient yeasts arrest in telophase and enter quiescence in response to nitrogen starvation.

IV. Discussion

Our results indicate that, during nitrogen starvation in *S. cerevisiae*, autophagy gene products are essential for cell cycle progression and G_1/G_0 arrest. However, these proteins are dispensable for acquisition of a quiescent phenotype, including acquisition of thermo-resistance and accumulation of storage carbohydrates. This requirement for autophagy genes is consistent with a previous report demonstrating that *atg2*Δ yeasts are deficient in G_2/M progression during starvation (Matsui et al., 2013). Our observation of a similar phenotype in yeast with null mutations in multiple other autophagy genes, including *ATG1*, *ATG5*, *VPS30/ATG6*, *ATG7* and *ATG8*, provides additional support for the finding that the autophagy pathway is essential in cell cycle progression following nitrogen starvation. Moreover, our results also demonstrate a somewhat unexpected finding – namely, that core autophagy genes are NOT essential for key aspects of starvation-induced cellular quiescence, at least in the budding yeast, *S. cerevisiae*. In addition, our results identify an as-of-yet undescribed block in cell cycle progression in autophagy-deficient yeasts during nitrogen starvation; based on analysis of spindle morphology, we found that *vps30*Δ/*atg6*Δ, *atg7*Δ, and *pep4*Δ yeasts arrest in telophase. Thus, in contrast to the findings of Matsui et al. which reported a role for Atg2 in recovery from a Swe1-dependent checkpoint and entry into mitosis (Matsui et al., 2013), our results demonstrate a role for autophagy in mitotic exit rather than mitotic entry.

The mechanism(s) by which autophagy genes are required for mitotic exit during nitrogen starvation are not yet fully understood. In the study by Matsui et al., it was postulated that starved cells rely on autophagy to generate catabolites necessary for synthesizing proteins essential for cell cycle progression; indeed, the defect in G_2/M progression in *atg2*Δ yeasts with auxotrophy for tryptophan is rescued when tryptophan is added to the nitrogen-depleted

medium (Matsui et al., 2013). However, in our study, it seems unlikely that the lack of cytoplasmic availability of amino acids, nucleic acids, and/or other catabolites is responsible for the defect in starvation-induced G_1/G_0 arrest as yeasts lacking the vacuolar permeases Atg22, Avt3 and Avt4 were similar to wild-type yeasts with respect to G_1/G_0 arrest in response to nitrogen starvation. It is possible that the role of nutrient recycling in G_2/M progression is different in a synchronous population following α-factor release (as studied by Matsui et al.) compared to the asynchronous population of yeasts examined in the present study. We also cannot definitively rule out a role for partially redundant unidentified vacuolar permeases other than Atg22, Avt3 and Avt4 in mediating mitotic exit in nitrogen starvation conditions.

In contrast to vacuolar permeases, we found that Pep4, a vacuolar protease required for autophagic cargo degradation,(Gerhardt et al., 1998) was required for proper starvation-induced G_1/G_0 arrest. This observation suggests two non-mutually exclusive potential mechanisms underlying the mitotic arrest phenotype which we observed in *vps30*Δ/*atg6*Δ, *atg7*Δ, and *pep4*Δ mutant yeasts. First, vacuolar protease-dependent autophagic protein degradation, in addition to ubiquitin-dependent mechanisms, may be required specifically in nitrogen starvation conditions (but not during normal growth conditions) for the well-characterized role of proteolysis in mitotic exit in *S. cerevisiae* (Hancioglu and Tyson, 2012; Weiss, 2012). A precedent for autophagy-dependent proteolysis of a cell cycle regulator in starvation but not nutrient-rich medium has already been provided for Swe1 in the study by Matsui et al. (Matsui et al., 2013). Further studies, beyond the scope of the present work, are required to determine whether a similar role for autophagy functions in nitrogen starvation in the degradation of proteins such as Clb2 and other molecules involved in the regulation of mitotic exit (Hancioglu and Tyson, 2012; Weiss, 2012; Yeong et al., 2000). A second

intriguing possibility is that, similar to the increasingly appreciated role of lysosomal nutrient sensing in regulating MTORC1 activity and other signaling pathways in mammalian cells (Betz and Hall, 2013; Efeyan et al., 2012), vacuolar nutrient sensing may regulate mitotic exit in yeast during nitrogen starvation.

The entry of autophagy-deficient yeasts into quiescence with 2N DNA content may have important implications for understanding broader aspects of yeast biology. First, since autophagy-deficient yeasts have impaired survival during nitrogen starvation (Tsukada and Ohsumi, 1993), our findings suggest that the quiescence program of autophagy-deficient yeasts is qualitatively different than the G_1/G_0 quiescence program in terms of permitting cells to adapt to nutrient deprivation. Second, it has been previously shown that yeasts that arrest in G_2/M have diminished ability to give rise to progeny (Daignan-Fornier and Sagot, 2011; Laporte et al., 2011; Wei et al., 1993), but the mechanistic basis for this has been unclear. Matsui et al. found that *atg2*Δ yeasts with a defect in G_2/M progression during nitrogen starvation have increased aneuploidy following replenishment with a nitrogen source and cell division (Matsui et al., 2013). Therefore, our findings, taken together with these previous observations, suggest a model in which entry into quiescence in G_2/M (such as that which occurs in autophagy-deficient yeasts) may increase genome instability, and thereby diminish production of progeny. Clearly, despite having similar markers of quiescence that signify similar adaptation to environmental stress (such as the acquisition of thermotolerance), there are fundamental as-of-yet undefined differences between G_1/G_0 and quiescence entry during other stages of the cell cycle that may explain the beneficial effects of G_1/G_0 quiescence on eukaryotic cell survival and reproduction.

V. Figures

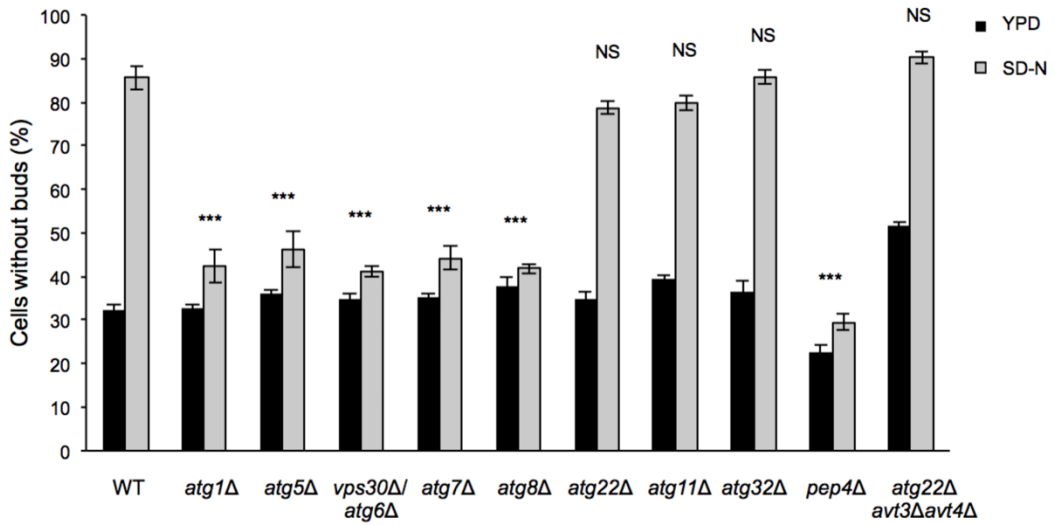

Figure 3. 1. Budding assay of wild-type and autophagy-deficient yeasts after 4 h of nitrogen starvation.

Quantification of the percentage of wild-type and indicated atg mutant yeast strains without buds at time 0 (YPD) or 4 h in SD-N (SD-N). Bars represent mean ± SEM of triplicate samples (at least 100 cells per sample were counted). Similar results were observed in more than 3 independent experiments. 2-way ANOVA with Bonferroni correction for comparison of magnitude of change between YPD and SD-N in the indicated atg mutant yeast strain compared to the magnitude of change between YPD and SD-N in wild-type (WT) yeasts.

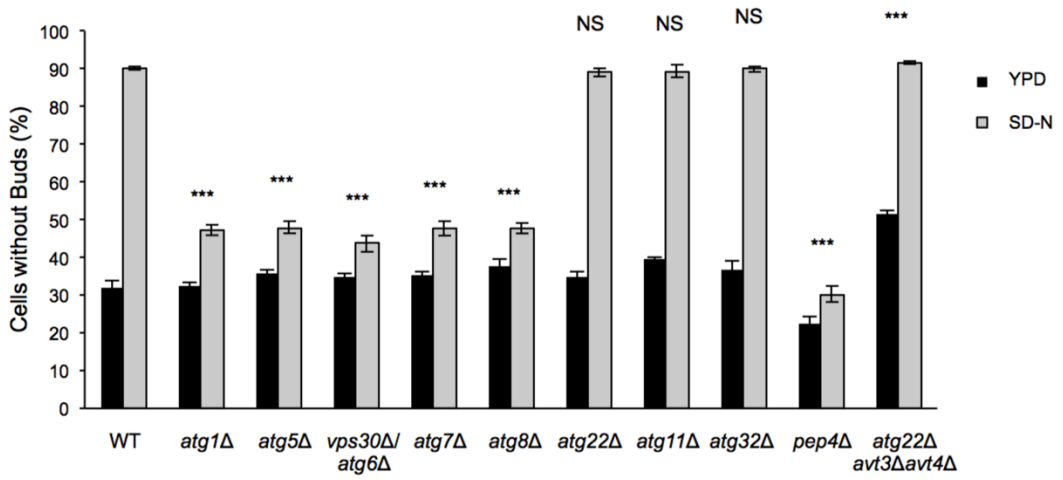

Figure 3. 2. Budding assay of wild-type and autophagy-deficient yeasts after 24 h of nitrogen starvation.

Quantification of the percentage of wild-type and indicated atg mutant yeast strains without buds at time 0 (YPD) or 24 h in SD-N (SD-N). Bars represent mean ± SEM of triplicate samples (at least 100 cells per sample were counted). Similar results were observed in more than 3 independent experiments. 2-way ANOVA with Bonferroni correction for comparison of magnitude of change between YPD and SD-N in the indicated atg mutant yeast strain compared to the magnitude of change between YPD and SD-N in wild-type (WT) yeasts.

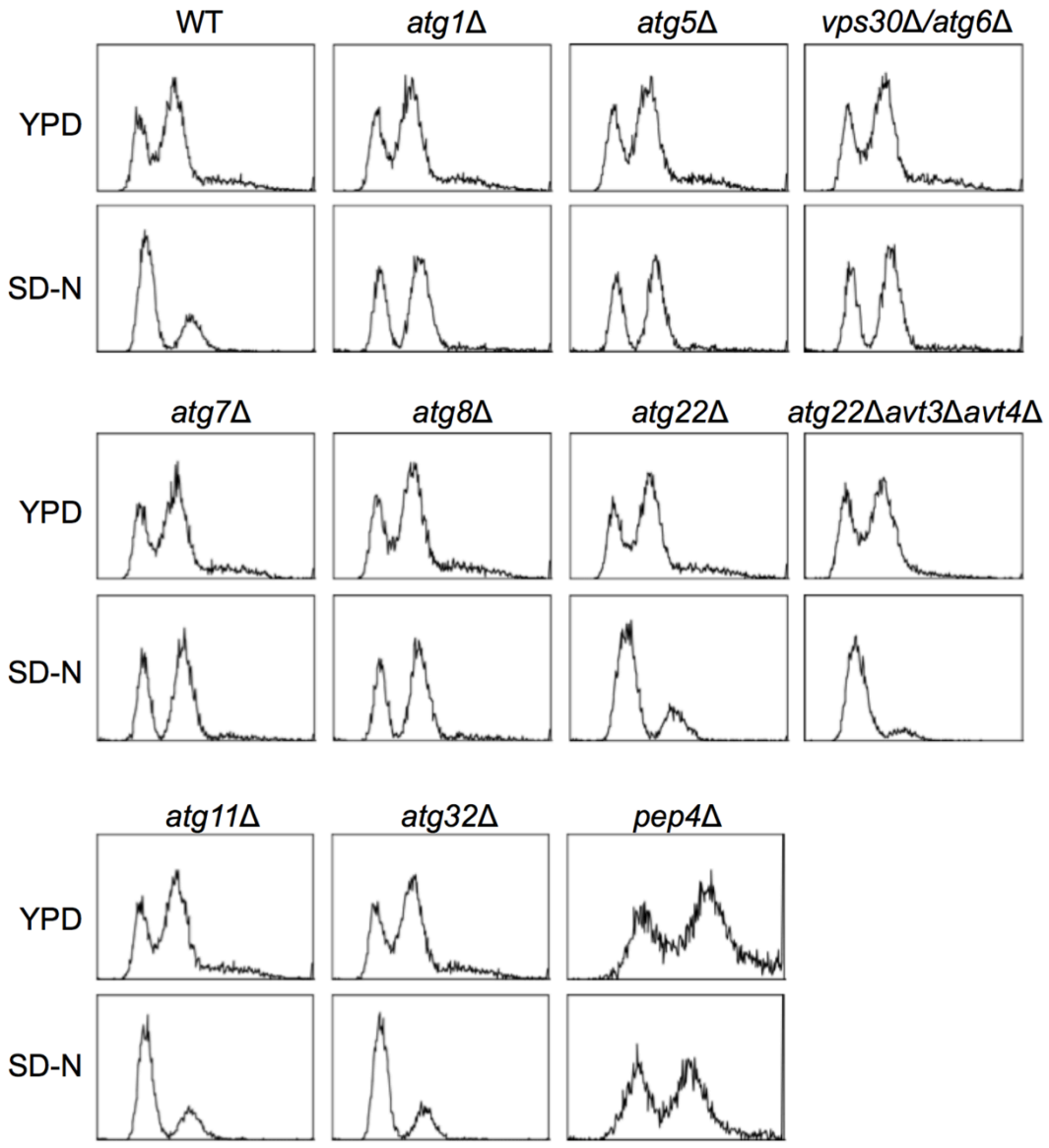

Figure 3. 3. FACS analysis of cell cycle of the indicated yeast strains after growth in YPD or SD-N for 4 h.

10,000 cells were analyzed per strain. Similar results were observed in more than 3 independent experiments.

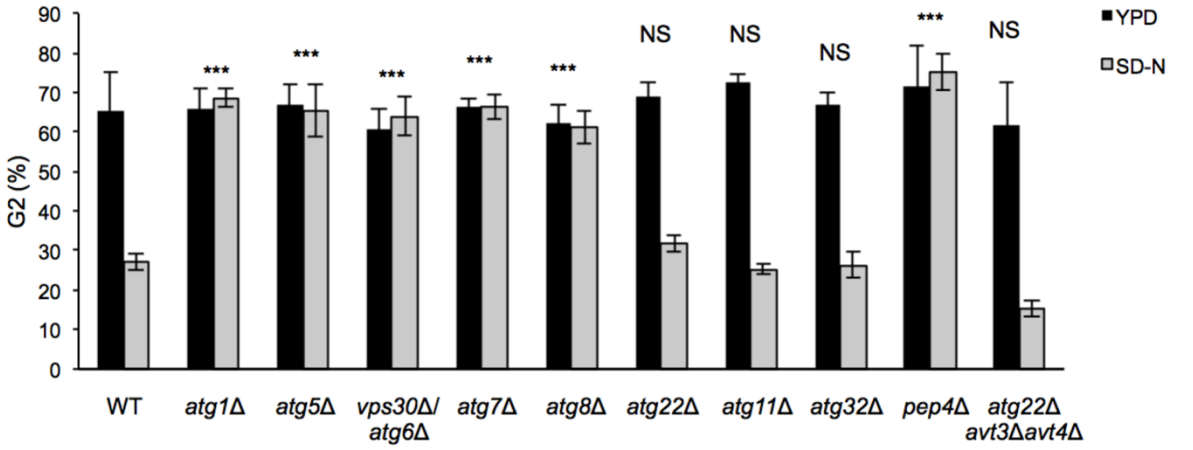

Figure 3. 4. FACS quantification of cell cycle of the indicated yeast strains after growth in YPD or SD-N for 4 h.

The flow cytometry data from three independent experiments were fitted to the Dean-Jet-Fox model and the percentage of cells in G2 was shown. *** P<0.001, NS, not significant; 2-way ANOVA with Bonferroni correction for comparison of magnitude of change between YPD and SD-N in the indicated atg mutant strain compared to the magnitude of change between YPD and SD-N in wild-type (WT) yeasts.

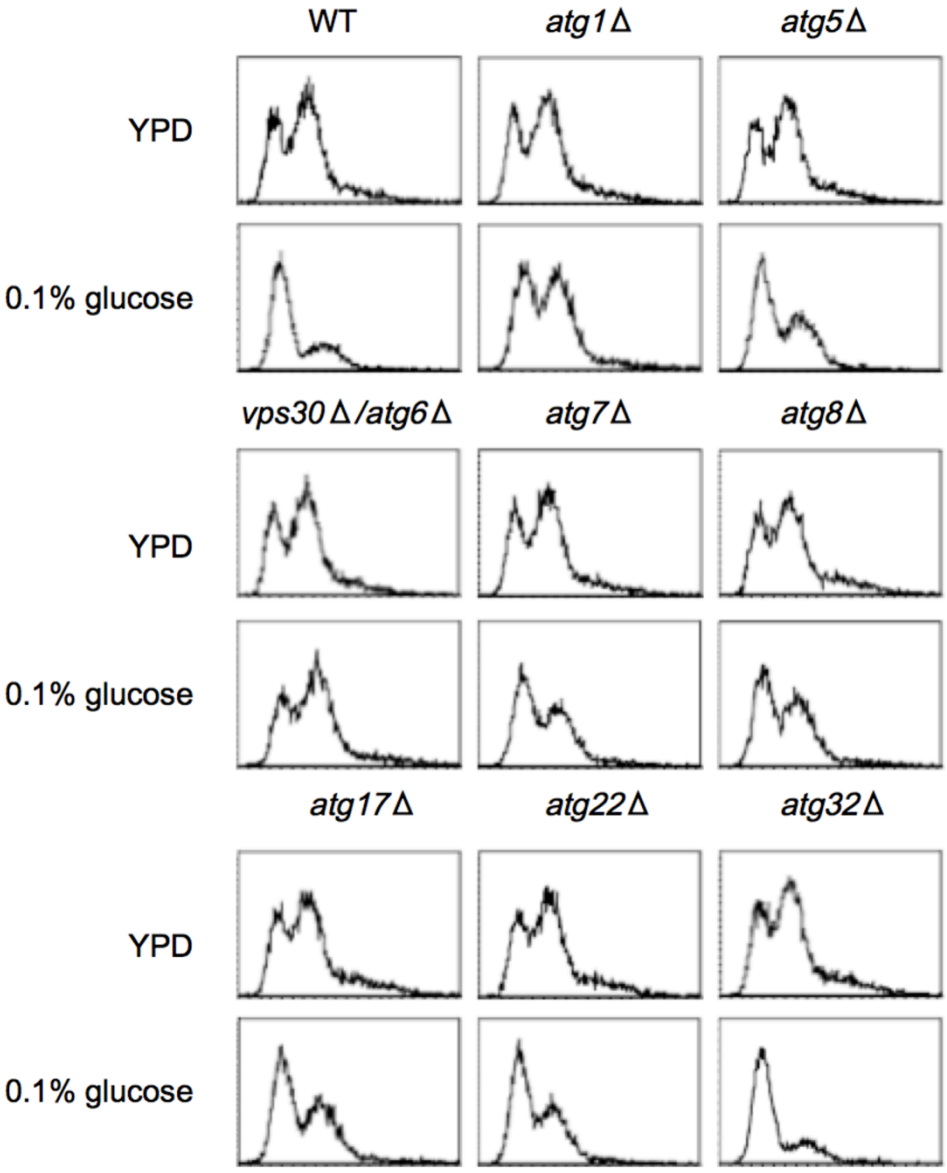

Figure 3. 5. FACS analysis of wild-type and autophagy-deficient yeasts during carbon starvation.

FACS analysis of cell cycle of the indicated yeast strains after growth in YPD or carbon starvation medium (0.1% glucose) for 4 h. 10,000 cells were analyzed per strain.

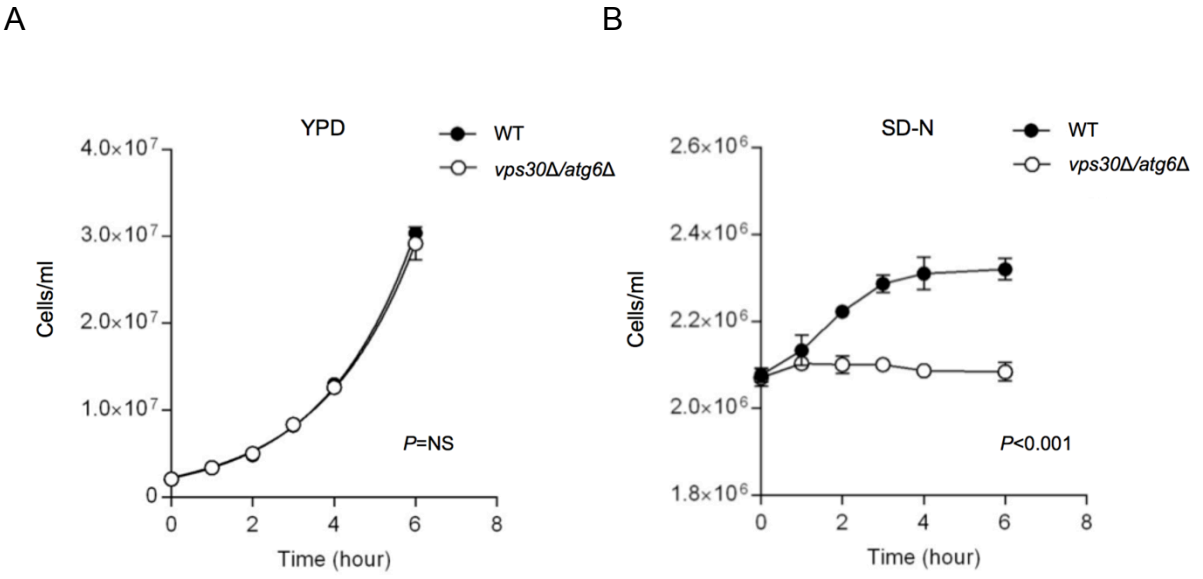

Figure 3. 6. Cell growth of wild-type and autophagy-deficient yeast during nitrogen starvation.

(A and B) Yeast cells grown in YPD were harvested, washed 3 times with autoclaved water and resuspended in YPD (A) or SD-N (B). Cell number was quantified at the time indicated using a hemocytometer. Values represent mean ± SEM of triplicate samples. Similar results were observed in 2 independent experiments. In (A) cell growth curves were fitted to an exponential growth model to determine their doubling time. The difference between growth curves in wild-type (WT) versus *vps30*Δ/*atg6*Δ yeast strains was analyzed using an ANOVA model; statistical results are indicated in each graph. NS, not significant.

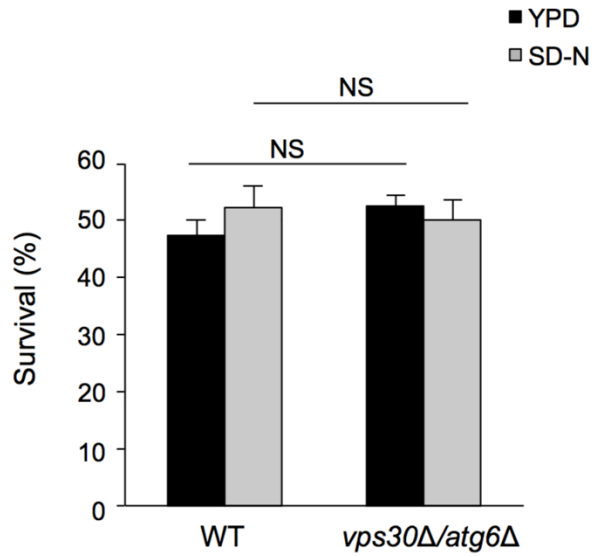

Figure 3. 7. Cell survival of wild-type and autophagy-deficient yeast during nitrogen starvation.

Wild-type (WT) and *vps30*Δ/*atg6*Δ strains were grown in YPD or SD-N for 4 h and tested for survival by plating 100 cells at 30°C for 48 h on YPD plates. Cell survival was calculated as the percentage of colonies over the total number of plated cells. Bars represent mean ± SEM of triplicate samples. Similar results were observed in 2 independent experiments. NS, not significant; 1-way ANOVA for indicated comparison.

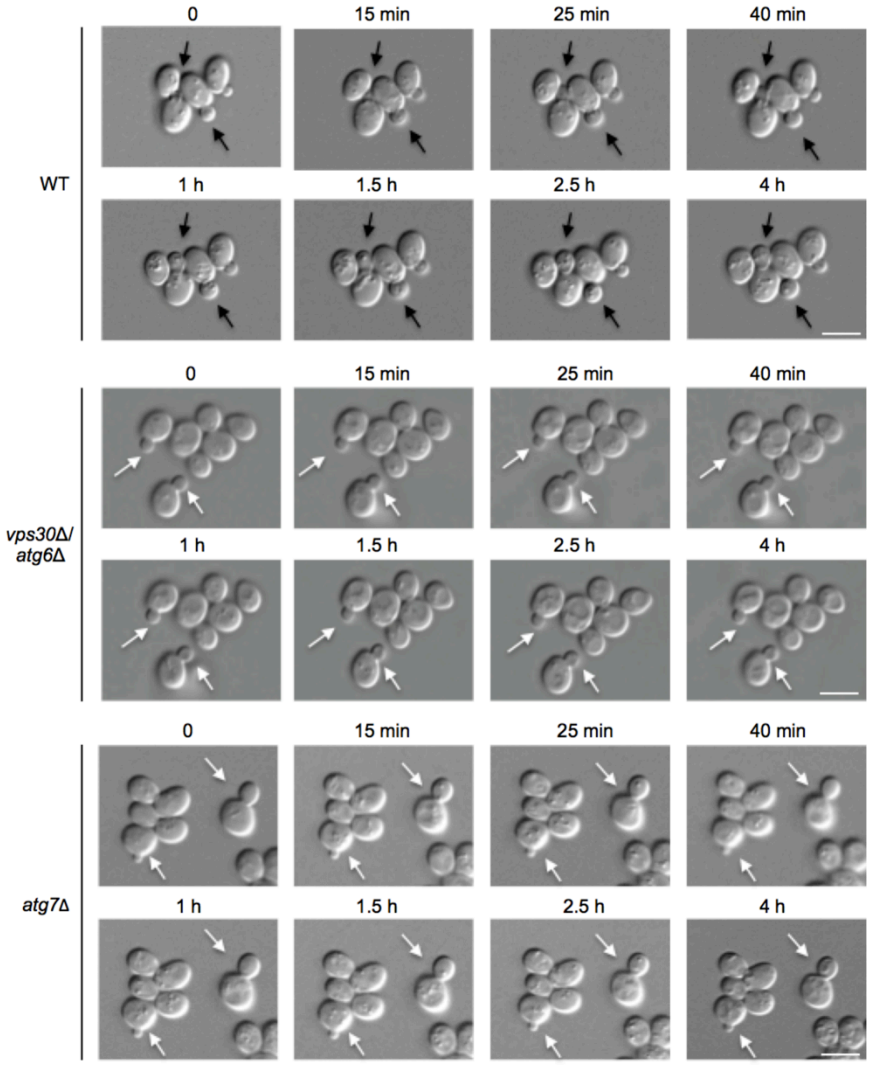

Figure 3. 8. Autophagy-deficient yeasts fail to complete cell division after nitrogen starvation.

Yeasts were grown on an SD-N agarose pad and images were taken at serial time points using a Carl Zeiss microscope. The time above each image indicates the time in nitrogen starvation (SD-N). Black arrows denote buds that separate to become daughter cells during the imaging period. White arrows denote buds that fail to separate to become daughter cells during the imaging period. Scale bar, 5 μm. At least 15 cells were examined and similar results were observed in at least 3 different experiments.

A

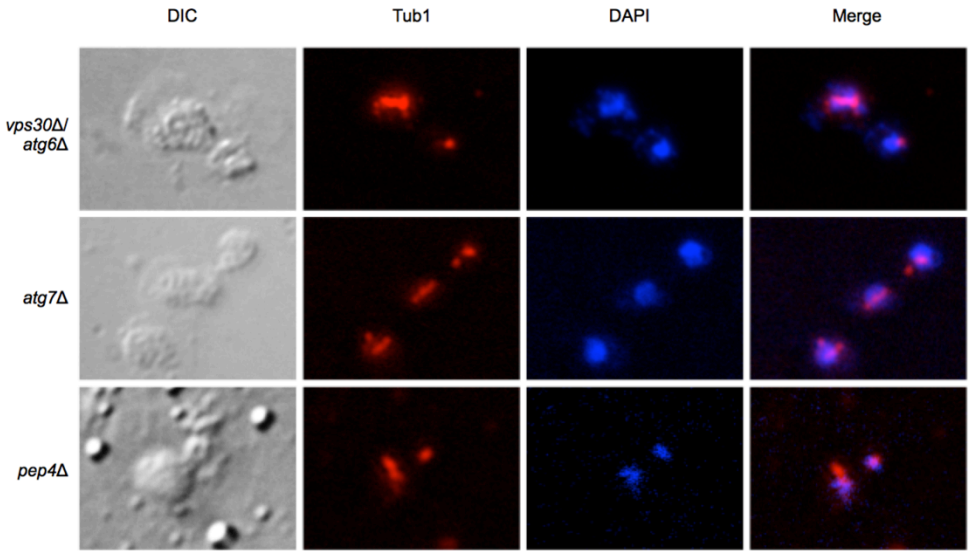

B

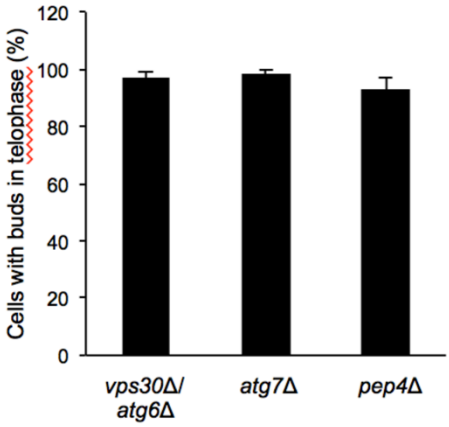

Figure 3. 9. Autophagy-deficient yeasts arrest in telophase after nitrogen starvation.

(A) Yeasts were starved in SD-N for 4 hs and stained with an antibody against Tub1. DNA was stained with DAPI. (B) Quantification of cells with buds in telophase. At least 50 cells were quantified and the experiment was done in triplicate. Bars represent mean ± SEM of triplicate samples. Similar results were observed in 3 independent experiments.

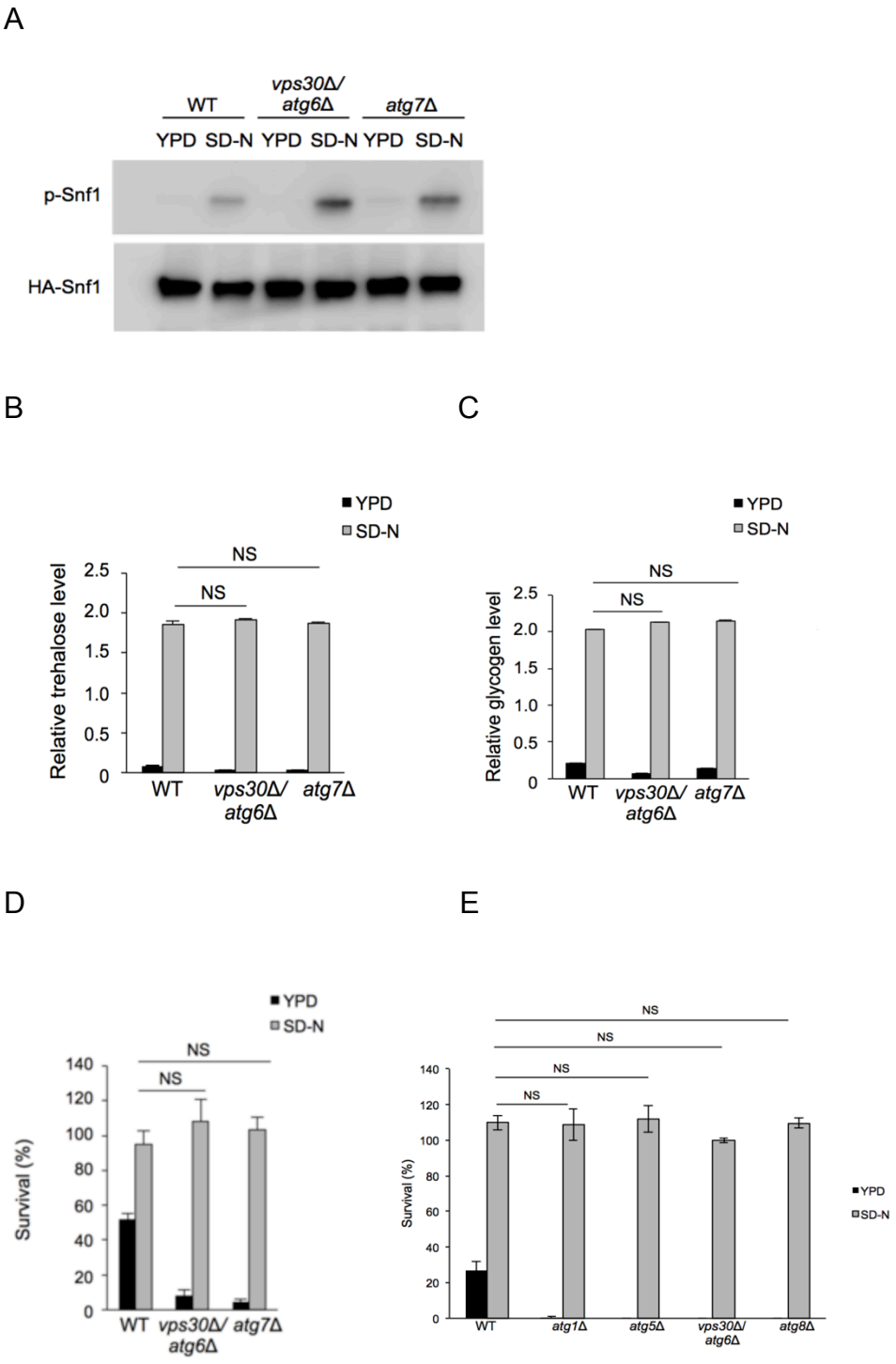

Figure 3. 10. Analysis of quiescence-specific phenotypes in wild-type and autophagy-deficient yeasts after nitrogen starvation.

(A) HA-Snf1 was transformed into the indicated yeast strains using the Frozen-EZ Yeast Transformation II Kit _(Zymo Research). Western blot detection of p-Snf1 was probed after in YPD (starting time point) or SD-N (30 min starvation). Similar results were observed in 3 independent experiments. (B and C) Measurement of trehalose (B) and glycogen (C) levels in yeasts grown in YPD or SD-N for 4 h. Bars represent mean ± SEM for triplicate samples. Similar results were observed in 3 independent experiments. (D) Assessment of heat shock-resistance in indicated yeast strains during growth in YPD or SD-N for 4 h. Bars represent mean ± SEM of triplicate samples. Similar results were observed in 3 independent experiments. NS, not significant; 1-way ANOVA with Tukey test for multiple comparisons.

CHAPTER FOUR

The regulation of Beclin 1 S90 phosphorylation and its role in autophagy

I. Abstract

Bcl-2 family members inhibit autophagy through binding to the BH3 domain of Beclin 1; however, the mechanisms by which Bcl-2 binding alters the autophagy function of Beclin 1 are not understood. Here we show that during starvation, Beclin 1 S90 is phosphorylated, which is essential for autophagy induction and tumor suppression. The phosphorylation is mediated by the stress-induced kinases, MAPAKAK2 and MAPAPK3 (MK2 and MK3). Experimental results in MK2/3 double-knockout MEF cells and Beclin 1 shRNA U2OS cells showed that MK2/MK3-mediated phosphorylation of Beclin 1 is required for starvation-induced autophagy. Starvation and constitutively active MK2-mediated Beclin 1 phosphorylation are blocked by Bcl-2 binding to Beclin 1. Moreover, mice with non-phosphorylatable knock-in mutations in Bcl-2 that prevent starvation-induced dissociation from Beclin 1 are resistant to starvation-induced Beclin 1 S90 phosphorylation and starvation-induced autophagy. Together, these findings identify MK2/MK3 as crucial stress signaling kinases that function in the positive regulation of autophagy through Beclin 1 phosphorylation, and identify the blockade of MK2-dependent Beclin 1 S90 phosphorylation as a mechanism by which Bcl-2 inhibits the autophagy function of Beclin 1.

II. Introduction

Beclin 1, the mammalian ortholog of yeast Atg6, is an essential protein in autophagy (Levine and Kroemer, 2008). It was originally discovered as a Bcl-2-interacting protein in a yeast two-hybrid screen (Liang et al., 1999). It regulates multiple physiological processes including tumorigenesis, development, apoptosis and neurodegeneration (Kang et al., 2011; Kroemer and Levine, 2008). In the Beclin 1/Vps34 complex, Beclin 1 functions as a platform recruiting activators or repressors of autophagy, and controls autophagosome formation through regulation of Class III PI3K activity (He and Levine, 2010). Endogenous Beclin 1 localizes to the trans-Golgi network, the mitochondria, the perinuclear membrane and the ER (Pattingre et al., 2005).

Beclin 1 is a multi-domain protein. It has a N-terminal domain, a Bcl-2-binding domain, a coiled-coil domain, an evolutionarily conserved domain which is essential for the interaction with Vps34, a BH3-only domain and a nuclear export signal. Beclin 1 can also form homodimers which favor the interaction with Bcl-2 and Rubicon.

In mammalian cells, the anti-apoptotic protein Bcl-2 interacts with Beclin 1 under nutrient-rich conditions and inhibits autophagy. Dissociation of Bcl-2 from Beclin 1 is a critical step for activating autophagy in response to starvation (Pattingre et al., 2005). c-Jun N-terminal kinase 1 (JNK1) phosphorylates Bcl-2 on T69, S70 and S87, which is required for its starvation-induced dissociation from Beclin 1 and autophagy activation (Wei et al., 2008).

However, how autophagy is activated after the dissociation of Bcl-2 from Beclin 1 remains to be answered.

The physiological function of Beclin 1 is tightly regulated by different kinases through phosphorylation. Beclin 1 phosphorylations are important in autophagy induction. AMPK phosphorylates Beclin 1 on S91 and S94 (S93 and S96 in human) during glucose starvation to promote autophagy (Kim et al., 2013). Ulk1 phosphorylates Beclin 1 on S14 (S16 in human) in response to amino acid starvation and this phosphorylation is required for VPS34 activation (Russell et al., 2013). DAPK phosphorylates Beclin 1 on T119, promoting the dissociation of Beclin 1 from Bcl-2-like proteins (Zalckvar et al., 2009). In contrast, phosphorylation of Beclin 1 can be important to repress excessive autophagy during growth-promoting conditions. Phosphorylation of Beclin 1 S234 and S295 by Akt inhibits autophagy and promotes tumorigenesis (Wang et al., 2012). Moreover, EGFR phosphorylates Beclin 1 on Y229, Y233 and Y352. Those phosphorylations reduce autophagy, enhance tumor growth and tumor dedifferentiation (Wei et al., 2013). These studies indicate that phosphorylation of Beclin 1 is important to regulate its physiological functions.

MAP kinase activated protein kinases (MAPKAPKs) are kinases activated by MAP kinases (MAPKs). There are three conserved subfamilies: MAPKAPK2 (containing MAPKAPK 2 and MAPKAPK 3), MNK and MK5 (MAPKAPK5). MAPKAPK 2 (MK2) and MAPKAPK 3 (MK3) share high sequence homology and functional redundancy (Gaestel, 2006). Both of them form a complex with and are activated by p38 MAP kinase. MK2 and MK3 play

critical roles in multiple pathways by phosphorylating substrates regulating cytokine and interferon production, cytoskeleton rearrangement and RNA stability. In a siRNA screen, knocking down MK2 increases GFP-LC3 dots (Szyniarowski et al., 2011). However, since there is compensation between MK2 and MK3 (Ronkina et al., 2007), it is still not clear if MK2/3 positively or negatively regulates autophagy.

Here we found MK2/3 phosphorylate Beclin 1 S90 during stress conditions such as starvation and high osmotic stress. S90 phosphorylation leads to autophagy induction and decreased human breast carcinoma cell anchorage-independent growth *in vitro* and tumor formation *in vivo*. The interaction between Bcl-2 and Beclin 1 inhibits S90 phosphorylation, providing a mechanism by which Bcl-2 inhibits autophagy. Moreover, we found that MK2/3 are novel positive regulators of autophagy. They positively regulate autophagy by phosphorylating Beclin 1 S90. We also identified AMPK and Atg14 as positive regulators of Beclin 1 S90 phosphorylation. We also found that osmotic stress induced Beclin 1 S90 phosphorylation is important for cell survival. Our study for the first time demonstrates a connection between MKs and Beclin 1 and demonstrates a potential mechanism by which the Bcl-2-Beclin 1 interaction negatively regulates autophagy induction.

III. Results

Beclin 1 serine 90 is phosphorylated and is induced by starvation

To identify new phosphorylation sites of Beclin 1, we performed mass spectrometry analysis of Flag epitope-tagged full-length Beclin 1 purified from SKNSH cells grown in nutrient-rich

or starvation conditions. As reported previously (Fogel et al., 2013), we also found that S90 was a phosphorylation site of Beclin 1 during starvation (data not shown) (**Fig. 4. 1A**). In HeLa cells transiently transfected with Flag-tagged Beclin 1 1-105 (**Fig. 4. 1B**) or full-length Flag-Beclin 1 (**Fig. 4. 2A**), following metabolic labeling with P^{33} and immunoprecipitation with an anti-Flag antibody, minimal phosphorylated Beclin 1 could be detected during nutrient-rich conditions. However, during starvation, Beclin 1 phosphorylation was potently induced (**Fig. 4. 2A**). Mutation of S90 to alanine almost abolished the P^{33} signal of Beclin 1, indicating that S90 is a major phosphorylation site induced after starvation (**Fig. 4. 2A**).

To confirm that Beclin 1 S90 is phosphorylated, we generated a phospho-specific antibody that recognizes Beclin 1 S90-P (**Fig. 4. 2A and 4. 2B**). We confirmed that Beclin 1 S90 phosphorylation is induced by nutrient starvation (**Fig. 4. 2A and 4. 2B**). Using this antibody, we also confirmed that nutrient starvation induced the phosphorylation of endogenous Beclin 1 S90 in Hela cells within 30 min (**Fig. 4. 2B**). These data indicate that S90 is a nutrient-responsive phosphorylation site of Beclin 1.

Beclin 1 serine 90 phosphorylation is required for autophagy induction

To evaluate the role of Beclin 1 S90 phosphorylation in autophagy regulation, we took advantage of MCF7 human breast carcinoma cells that have a monallelic deletion of *beclin 1* (Pattingre et al., 2005). In MCF7 cells, starvation-induced autophagy is deficient due to low endogenous Beclin 1 expression levels. We co-expressed GFP-LC3 and Beclin 1 constructs and autophagosome numbers were measured by quantifying the number of GFP-LC3 dots

per cell. As reported (Pattingre et al., 2005), enforced expression of wild-type Beclin 1 restored starvation-induced autophagy in MCF7 cells. The Beclin 1 S90A mutant failed to induce autophagy in response to starvation (**Fig. 4. 3**), indicating that Beclin 1 S90 phosphorylation is essential for autophagy induction in response to nutrient starvation. In contrast, a phosphorylation mimic mutant Beclin 1 S90E significantly increased GFP-LC3 dot numbers in basal conditions, suggesting that Beclin 1 S90 phosphorylation may be sufficient to induce autophagy (**Fig. 4. 3**).

To evaluate the functions of Beclin 1 S90 mutants in autophagy in an independent cell line, we used *beclin 1* shRNA U2OS cells in which endogenous Beclin 1 protein expression can be silenced by doxycycline treatment-inducible shRNA expression (Sun et al., 2008). As shown previously, after doxycycline treatment, the *beclin 1* shRNA U2OS cells were deficient in starvation-induced autophagy which was rescued by overexpression of shRNA non-targetable wild-type Beclin 1 (**Fig. 4. 4A**). Consistent with our observations in MCF7 cells, the shRNA non-targetable Beclin 1 S90A mutant failed to induce autophagy in response to starvation (**Fig. 4. 4A**). This result confirmed that Beclin 1 S90 phosphorylation is essential for autophagy induction after starvation. The shRNA non-targetable phosphorylation mimic mutant Beclin 1 S90E significantly increased GFP-LC3 dot number in basal conditions, confirming that Beclin 1 S90 phosphorylation is sufficient to induce autophagy (**Fig. 4. 4A**). The increase in GFP-LC3 dot numbers was not due to a blockade of autophagosome-lysosome fusion because bafilomycin treatment further increased GFP-LC3 dot number in all samples examined (**Fig. 4. 4A**). In addition, differences in levels of

autophagy were not due to differences in levels of Beclin 1 protein expression, as western blot analysis showed comparable levels of expression in cells transfected with the different shRNA-resistant Beclin 1 mutant constructs (**Fig. 4. 4B).**

Beclin 1 serine 90 is essential for the tumor suppressing function of Beclin 1

Beclin 1 is a haplo-insufficient tumor suppressor (Qu et al., 2003; Yue et al., 2003). To test whether Beclin 1 S90 is required for its tumor suppressor function, we assessed whether Beclin 1 S90 is important in regulating tumor growth. We stably expressed exogenous Flag-Beclin 1 constructs in MCF-7 cells and the Beclin 1 expression levels among different mutants were comparable (**Fig. 4. 5A**). We performed xenograft studies in immunodeficient *nu/nu* mice. As expected, MCF-7 cells that stably express wild-type Beclin 1 grew slower than MCF-7 cells transfected with an empty vector control (**Fig. 4. 5B**). MCF-7 cells that stably express Beclin 1 S90E grew at comparable rates as MCF-7 cells that express wild-type Beclin 1. Of note, MCF-7 cells that stably express Beclin 1 S90A grew at a comparable rate as MCF-7 vector control cells (**Fig. 4. 5B**). These data indicate that the Beclin 1 S90 site is required for its tumor suppressor function.

Beclin 1 serine 90 is phosphorylated by MK2/3

Next, we sought to identify the upstream kinase(s) that mediate starvation-induced phosphorylation of Beclin 1 S90. We performed a kinase screen using a 15 amino acid peptide derived from Beclin 1 containing S90 and seven flanking residues on each side. An

in vitro kinase assay was performed using a kinase pool consisting of 190 serine/threonine kinases. MK3 was identified as the only kinase in the pool that has significant kinase activity against the Beclin 1 peptide (data not shown). Since there are other serine and threonine residues in the peptide, we performed a mutational analysis. MK3 only showed kinase activity using the wild-type peptide but not the S90A or S90A/S93A/S96A mutant peptides as a substrate. This result suggests that Beclin 1 S90 is an essential serine residue in the peptide for MK3-dependent phosphorylation (**Fig. 4. 6A**).

MK3 is highly homologous to MK2, another MAP kinase-activated protein kinase. Both kinases can be activated by p38 in a stress-dependent manner. They share 75% sequence identity and showed functional redundancy (Gaestel, 2006). The expression level of MK2 is significantly higher than that of MK3 in different tissues and cells; therefore, we wanted to test whether MK2 also phosphorylates Beclin 1 S90. MK2 also phosphorylated the Beclin 1 S90-containing peptide, although the kinase activity of MK2 was lower than that of MK3 (**Fig. 4. 6B**). MK5 did not show any kinase activity to the Beclin 1 S90-containing peptide. We also examined the *in vitro* kinase activity of MK2 and MK3 using Flag-Beclin 1 purified from HeLa cells as a substrate. In this *in vitro* kinase assay, both MK2 and MK3 exhibited similar kinase activity in phosphorylating Beclin 1 S90 (**Fig. 4. 6C**).

To investigate whether MK2 phosphorylates Beclin 1 S90 in cultured cells, we overexpressed dominant-negative and constitutively active MK2 in HeLa cells. While dominant negative MK2 almost completely blocked starvation-induced Beclin 1 S90

phosphorylation, constitutively active MK2 greatly increased Beclin 1 S90 phosphorylation during nutrient-rich conditions (**Fig. 4. 7A**), indicating that MK2 phosphorylates Beclin 1 S90 in cultured cells. Phosphorylation of Hsp27 was used as an indicator of MK2 activity (**Fig. 4. 7A**).

To further confirm that MK2/3 phosphorylate Beclin 1 S90 *in vivo*, we examined S90 phosphorylation in MK2/MK3 double-knockout cells. As shown previously, starvation strongly induced Beclin 1 S90 phosphorylation in the wild-type MEFs (data not shown). However, in MK2/3 double knockout MEFs, starvation-induced Beclin 1 S90 phosphorylation is greatly diminished, and this is rescued by overexpression of MK2 (**Fig. 4. 7B**). Taken together, these results suggest that MK2 and MK3 are the kinases that phosphorylate Beclin 1 S90 in response to nutrient starvation.

Previous studies have shown that MK2 is activated by multiple stimuli such as LPS treatment and osmotic stress (Gaestel, 2006), which are stimuli that we showed also result in Beclin 1 S90 phosphorylation (**Fig. 4. 16B and 4. 16C**). However, it was not previously known whether MK2 can be activated by starvation, a crucial stimuli leading to MK2/MK3-dependent Beclin 1 S90 phosphorylation. Indeed, we found that starvation led to a band shift of MK2 (**Fig. 4. 10B and 4. 10C**) and increased phosphorylation of the downstream substrate, Hsp27 (**Fig. 4. 7A**, **Fig. 4. 10B and 4. 10C**), indicating that MK2 is activated.

MK2 positively regulates autophagy

In a previous siRNA screen study, MK2 was identified as a negative regulator of autophagy (Szyniarowski et al., 2011). However, since decreased levels of MK2 will lead to increased expression of MK3, the effects of MK2/3 on autophagy regulation are not well-understood. We used dominant negative MK2 (which blocks the kinase activity of both MK2 and MK3), constitutively active MK2, and MK2/3 double knockout MEFs to further explore this question. As measured by the number of GFP-LC3 dots per cell (**Fig. 4. 8A**), dominant-negative MK2 suppressed starvation-induced autophagy and constitutively active MK2 increased basal autophagy. In MK2/3 double-knockout MEF cells compared to MK2/3 double-knockout MEFs reconstituted with MK2, both basal and starvation-induced autophagic flux was decreased (**Fig. 4. 8B**). These results together indicate that MK2 is a positive regulator of autophagy.

MK2/3 positively regulate autophagy by phosphorylating Beclin 1 S90

To evaluate whether MK2/3 positively regulate autophagy by phosphorylating Beclin 1 S90, we first wanted to test the hypothesis that Beclin 1 S90E, but not Beclin 1 S90A, would increase autophagy in MK2/3 double knockout MEFs. We infected the MK2/3 double-knockout MEFs with retroviruses bearing the vector control, wild-type Beclin 1, Beclin 1 S90A or Beclin 1 S90E constructs and measured autophagy levels by quantifying GFP-LC3 dots per cell. We found that in Beclin 1 S90E expressing cells, both basal and starvation-induced autophagy was significantly increased compared with wild-type and Beclin 1 S90A

expressing cells (**Fig. 4. 9A**), indicating that a Beclin 1 S90 phosphorylation mimic can substitute for MK2/MK3 in autophagy upregulation. These results are consistent with a model in which MK2/3 regulate autophagy through phosphorylating Beclin 1 S90.

To more directly test the hypothesis that MK2/3 regulate autophagy by phosphorylating Beclin 1 S90, we co-expressed control vector, shRNA resistant Beclin 1 wild-type or Beclin 1 S90A together with vector control or constitutively active MK2 in doxycycline-inducible *beclin 1* shRNA U2OS cells. Constitutively active MK2 induced p62 degradation in wild-type Beclin 1 reconstituted cells but not in vector or Beclin 1 reconstituted cells (**Fig. 4. 9B**). These data demonstrate that MK2-induced upregulation of autophagy requires the Beclin 1 S90 phosphorylation site.

Bcl-2 negatively regulates MK2/3-mediated Beclin 1 serine 90 phosphorylation

Bcl-2 is a critical negative regulator of autophagy by interacting with Beclin 1. S90 is in the Bcl-2 binding domain of Beclin 1 (amino acids 88-150) (Oberstein et al., 2007). We therefore examined whether Bcl-2 overexpression would alter the phosphorylation status of Beclin 1 S90. Metabolic labeling showed that Bcl-2 overexpression greatly reduced the overall phosphorylation levels of Beclin 1 (**Fig. 4. 10A**). Since S90 is a major phosphorylation site of Beclin 1, we wanted to test whether the interaction between Bcl-2 and Beclin 1 would directly block the MK2-dependent phosphorylation of Beclin 1 S90. Therefore, we performed an *in vitro* kinase assay of MK2-dependent Beclin 1 phosphorylation in the presence of increasing amounts of recombinant purified GST-Bcl-2.

Our results showed that Bcl-2 blocked active MK2-mediated Beclin 1 S90 phosphorylation in a concentration-dependent manner (**Fig. 4. 10B**). In HeLa cells that stably overexpress Bcl-2, there was a delay in starvation induced Beclin 1 S90 phosphorylation and starvation-induced autophagy; increased Beclin 1 S90 phosphorylation, increased LC3-II conversion, and increased p62 degradation was observed at 2 h after starvation in parallel with disruption of the Bcl-2/Beclin 1 complex, but not at earlier time points. In contrast, in HeLa cells that stably express a Bcl-2 AAA mutant that does not disassociate from Beclin 1 after starvation, no starvation-induced Beclin 1 S90 phosphorylation or starvation-induced autophagy was observed (**Fig. 4. 10C**). In addition, overexpression of wild-type Bcl-2 partially blocked active MK2-mediated Beclin 1 S90 phosphorylation and autophagy, whereas overexpression of the Bcl-2 AAA mutant completely blocked active MK2-mediated Beclin 1 S90 phosphorylation as well as active MK2-induced autophagy (**Fig 4. 10D**). These data suggest that the binding of Bcl-2 to Beclin 1 inhibits MK2-mediated Beclin 1 S90 phosphorylation, and provide a biochemical mechanism by which Bcl-2 inhibits the autophagy function of Beclin 1.

To evaluate whether the interaction between Bcl-2 and Beclin 1 negatively regulates Beclin 1 S90 phosphorylation *in vivo*, we evaluated Beclin 1 S90 phosphorylation in the muscles of wild-type and Bcl-2 AAA mice following a 48 h starvation period. While starvation strongly induced Beclin 1 S90 phosphorylation and autophagy in the muscles of wild-type mice, both starvation-induced Beclin 1 S90 phosphorylation and autophagy was impaired in the muscles of Bcl-2 AAA mice (**Fig 4. 11**). Taken together, our *in vitro* and *in vivo* data indicate that

Bcl-2 binding to Beclin 1 inhibits MK2-dependent starvation-induced Beclin 1 S90 phosphorylation and autophagy.

We also examined whether overexpression of Beclin1 S90E would be able to bypass autophagy suppression mediated by Bcl-2 AAA. We co-transfected GFP-LC3 with either vector control or Beclin 1 wild-type, Beclin 1 S90A or Beclin 1 S90E into wild-type or Bcl-2 AAA MEFs and quantified the number of GFP-LC3 dots per cell. Bcl-2 AAA MEFs were deficient in starvation-induced autophagy, and this was rescued by overexpression of wild-type Beclin 1, presumably because of the lack of adequate levels of Bcl-2 to bind to overexpressed wild-type Beclin 1. In contrast, overexpression of Beclin 1 S90 did not rescue starvation-induced autophagy in Bcl-2 AAA MEFs, which would be predicted based on our earlier observations that S90 phosphorylation of Beclin 1 is essential for starvation-induced autophagy. The overexpression of Beclin 1 S90E increased basal autophagy in Bcl-2 AAA MEFs, indicating that this Beclin 1 S90 phosphorylation mimic mutant functions as a constitutively active mutant even when endogenous Beclin 1 function is inhibited by Bcl-2 AAA binding (**Fig 4. 12**).

Next we tested if Beclin 1 S90 phosphorylation will impair its interaction with Bcl-2. We found that both the Beclin 1 S90A and the Beclin 1 S90E mutants interact equally well with Bcl-2 as does wild-type Beclin 1, indicating that Beclin 1 S90 phosphorylation likely does not facilitate the dissociation of Beclin 1 from Bcl-2 (**Fig 4. 13**). Rather, the dissociate of

Beclin 1 from Bcl-2 likely allows Beclin 1 phosphorylation at S90 and subsequent autophagy induction.

Atg14 is essential for Beclin 1 serine 90 phosphorylation

It was reported that knockdown of Atg14 significantly decreases the phosphorylation of Beclin 1 (Fogel et al., 2013). However, the exact phosphorylation site is not clear. We tested whether Atg14 is essential for Beclin 1 S90 phosphorylation. Starvation induced Beclin 1 S90 phosphorylation in control U2OS cells. With Atg14 knocked-down, starvation-induced Beclin 1 S90 phosphorylation reduced to nearly undetectable. (**Fig 4. 14**). These data indicate that Atg14 is essential for starvation-induced Beclin 1 S90 phosphorylation.

Beclin 1 serine 93 phosphorylation regulates Beclin 1 serine 90 phosphorylation

AMPK phosphorylates Beclin 1 at serine 93 and serine 96, which induces autophagy after glucose starvation (Kim et al., 2013). Beclin 1 S90 is in close proximity to these sites and it is possible that there is some crosstalk among these sites. Interestingly, mutating S93 to alanine reduces starvation-induces Beclin 1 S90 phosphorylation (**Fig. 4. 15A**), indicating phosphorylation of Beclin 1 S93 may be contribute to the phosphorylation of Beclin 1 S90.

Since phosphorylation of Beclin 1 S93 is mediated by AMPK, we tested if AMPK regulates Beclin 1 S90 phosphorylation. Interestingly, active AMPK phosphorylates Beclin 1 S90 in

in vitro kinase assay (**Fig. 4. 15B**). Taken together, AMPK may be a positive regulator of Beclin 1 S90 phosphorylation.

Beclin 1 S90 phosphorylation is induced by multiple stressors.

S90 phosphorylation is also strongly induced by a previously reported autophagy-inducing peptide derived from a short fragment in the ECD domain of Beclin 1 (**Fig. 4. 16A**) (Shoji-Kawata et al., 2013). A point mutant of this peptide (Tat-Beclin 1 F270S), which cannot induce autophagy (Shoji-Kawata et al., 2013), fails to induce Beclin 1 S90 phosphorylation (**Fig. 4. 16A**). Excess concentrations of non-essential amino acids repress S90 phosphorylation (**Fig. 4. 16A**). Since MK2 is activated by osmotic stress and LPS treatment (Gaestel, 2006), we also tested if those stimuli would lead to induction of Beclin 1 S90 phosphorylation. We found that osmotic stress and LPS treatment also potently induce Beclin 1 S90 phosphorylation (**Fig. 4. 16B and 4. 16C**).

Beclin 1 S90 phosphorylation promotes cell survival under high osmotic stress

Excessive NaCl is one of the strongest known activators of MK2/3 and we found that it potently induces Beclin 1 S90 phosphorylation within minutes (**Fig. 4. 17A**). Additionally, other osmotic stress inducers such as sorbitol, sucrose or mannitol also activate MK2 and dramatically induce Beclin 1 S90 phosphorylation（**Fig. 4. 16B**). To test whether MK2 is essential for high osmotic stress-induced Beclin 1 S90 phosphorylation, we overexpressed a dominant negative MK2 mutant and found that high osmotic stress-induced Beclin 1 S90

phosphorylation was blocked (**Fig. 4. 17B**). In the MK2/MK3 double-knockout MEFs, high osmotic stress-induced Beclin 1 S90 phosphorylation was greatly diminished (**Fig. 4. 17C**). These data indicate that high osmotic stress-induced Beclin 1 S90 phosphorylation is mediated by MK2.

The kidney, while concentrating the urine, is under high osmotic stress. We found that in the mouse kidney cell line mIMCD3, high osmotic stress dramatically induced Beclin 1 S90 phosphorylation (**Fig. 4. 18A**). To further investigate if Beclin 1 S90 phosphorylation occurs *in vivo*, we stained mouse kidney sections with a Beclin 1 S90 phosphospecific antibody. Phospho-Beclin 1 S90 mainly localized in the collecting ducts and the vascular bundles in the medulla where osmotic stress is high (**Fig. 4. 18B and 4. 18C**). These data suggest that Beclin 1 S90 phosphorylation occurs in the kidney *in vivo* in regions of high osmotic stress.

High osmotic stress activates autophagy within minutes (**Fig. 4. 16B**). To evaluate whether osmotic stress-induced autophagy is mediated by MK2/3, we expressed vector control or dominant-negative MK2 in HeLa-GFP-LC3 cells. While osmotic stress induces autophagy in vector-transfected cells, dominant-negative MK2 expression significantly reduced osmotic stress-induced autophagy (**Fig. 4. 19**). These results suggest that osmotic stress induced autophagy is mediated by MK2.

Because autophagy is a critical pro-survival pathway, we also investigated whether Beclin 1 S90 phosphorylation is important for cell survival in response to high osmotic stress. We

stably transfected MK2/3 double-knockout MEFs with control vector, wild-type Beclin 1, Beclin 1 S90A, or Beclin 1 S90E and examined cell survival after exposure to high concentrations of NaCl. While the enforced expression of Beclin 1 S90A did not show any protection, the enforced expression of Beclin 1 S90E increased cell survival (**Fig. 4. 20**). These data indicate that Beclin 1 S90 phosphorylation may be required for cell survival in response to high osmotic stress.

IV. Discussion

Bcl-2 is a well-known negative regulator of autophagy. It interacts with Beclin 1 during nutrient-rich condition and inhibits autophagy (Pattingre et al., 2005). In response to starvation, Bcl-2 is phosphorylated by JNK1 at T69, S70 and S87, which leads to its dissociation from Beclin 1 (Wei et al., 2008). However, the mechanism by which Bcl-2 blocks autophagy and how autophagy is induced when Bcl-2 is dissociated from Beclin 1 remains elusive.

In this study, we provide a potential explanation for how the interaction between Beclin 1and Bcl-2 regulates autophagy. Under nutrient-rich conditions, Bcl-2 binds to Beclin 1 and blocks Beclin 1 S90 phosphorylation. Since Beclin 1 S90 phosphorylation is essential for autophagy induction, autophagy is inhibited when Bcl-2 is bound to Beclin 1. In response to starvation, JNK1 phosphorylates Bcl-2 and leads to its dissociation form Beclin 1. MK2/3 are activated by starvation and phosphorylate Beclin 1 S90, which, in turn, activates autophagy.

It was reported that only ER-localized Bcl-2 inhibits autophagy (Pattingre et al., 2005). It will be interesting to investigate whether only ER-localized Bcl-2 is able to inhibit Beclin 1 S90 phosphorylation. Moreover, we found that Atg14 is essential for Beclin 1 S90 phosphorylation. It is possible that only Atg14-associated Beclin 1 can be phosphorylated on residue S90. Moreover, whether Beclin 1 S90 phosphorylation alters the interactions between Beclin 1 and other binding partners is unknown. Additionally, whether Beclin 1 S90 phosphorylation leads to changes in the localization of Beclin 1 is not clear. Further studies need to be done to clarify these questions.

In this study, we also identified MK2/3 as newly described positive regulators of autophagy. This result contradicts the results from a previous siRNA screen in which MK2 was identified as a negative regulator of autophagy (Szyniarowski et al., 2011). However, it has been reported that loss of MK2 leads to transcriptional up-regulation of MK3 (Gaestel, 2006). Therefore, the induction of GFP-LC3 dots observed in the screen by knocking down MK2 may due to the transcriptional induction of MK3. Additionally, siRNAs may have off-target effects. To avoid the compensatory effect of MK3, we evaluated autophagy in MK2/3 double knockout MEF cells. We found that starvation-induced autophagy was impaired in MK2/3 double knockout MEFs compared to MK2/3 double knockout MEFs reconstituted with MK2. Additionally, a negative interfering mutant of MK2 ($MK2_{K76R}$) (Winzen et al., 1999) blocked starvation induced autophagy and a constitutively active mutant of MK2

($MK2_{EE}$) (Winzen et al., 1999) induced basal autophagy. Taken together, we showed that MK2 is a positive regulator of autophagy.

We noticed that in MK2/3 double knockout cells, starvation-induced and osmotic stress-induced S90 phosphorylation is not completely abolished, indicating that there are other kinases that can phosphorylate this site (or that are activated in a compensatory manner in the setting of MK2/3 deficiency). Considering the importance of Beclin 1 S90 phosphorylation in autophagy induction, it is not surprising that cells may utilize other kinases or pathways to phosphorylate Beclin 1 S90 when MK2/3 are absent. Our *in vitro* kinase assays using Beclin 1 immunoprecipitated from cells as a substrate showed that MK5 and AMPK could also phosphorylate Beclin 1 S90. However, since we did not see any kinase activity of MK5 or AMPK using the Beclin 1 S90 peptide as a substrate, it is very possible that the activity is indirect. Additional work is required to clarify whether MK5 or AMPK phosphorylates Beclin 1 S90. Moreover, other kinases that directly phosphorylate Beclin 1 S90 need to be identified.

It was recently reported that Beclin 1 S93 is phosphorylated by AMPK (Kim et al., 2013). We found that S93 phosphorylation regulates starvation induced S90 phosphorylation. AMPK may also positively regulate Beclin 1 S90 phosphorylation in cultured cells, although the effect, if present, is very small. However, whether AMPK regulates Beclin 1 S90 phosphorylation through phosphorylating Beclin 1 93 or Beclin 1 96 is not clear.

Understanding the coordination among different kinases and phosphorylation events during nutrient rich and stress conditions requires further study.

As an essential phosphorylation site of Beclin 1 in autophagy induction, the physiological function of Beclin 1 S90 phosphorylation needs to be further investigated. Although the *beclin 1* shRNA U2OS cells are helpful to study the role of Beclin 1 S90 phosphorylation, the creation of Beclin 1 S90A and S90E knock-in mice will be of great value for future investigation of the physiological functions of this phosphorylation site.

V. Figures

A

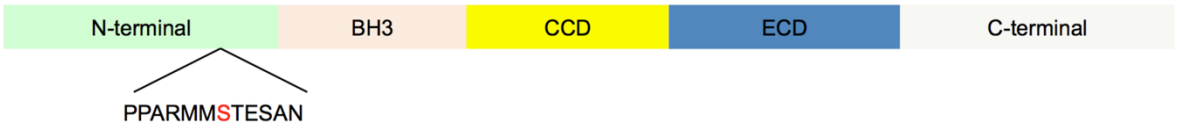

B

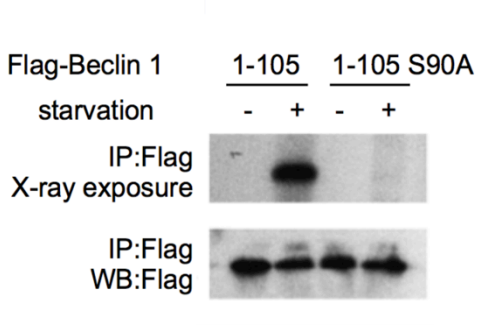

Figure 4. 1. Beclin 1 S90 is phosphorylated in response to starvation.

(A) S90 is located in the N-terminal domain of Beclin 1. (B) Detection by radioactive phosphate metabolic labeling of phosphorylated Flag-tagged Beclin 1 N-terminal fragment 1-105 and Beclin 1 1-105 S90A in HeLa cells. Western blot analysis was performed using an antibody against Flag. One representative example of 2 independent experiments is shown.

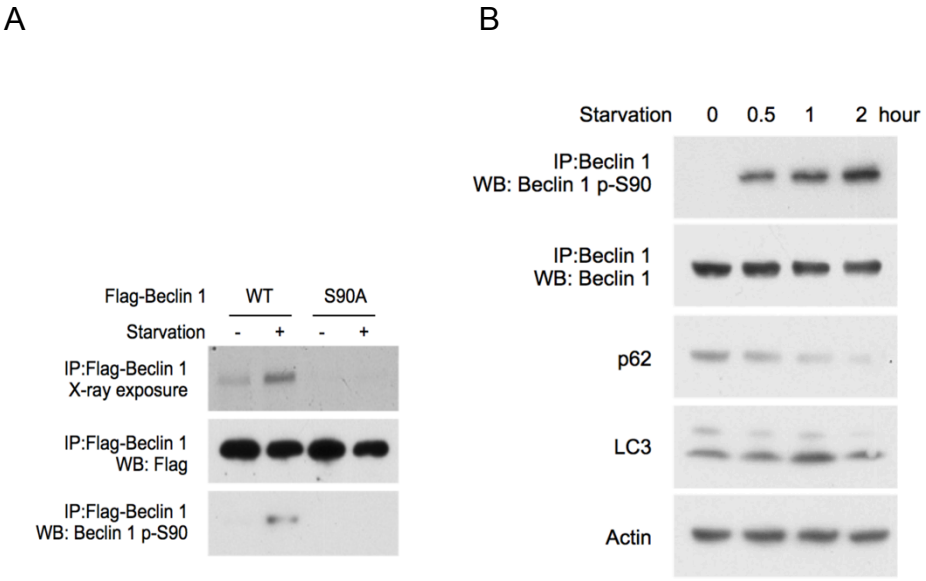

Figure 4. 2. Beclin 1 S90 is recognized by a phospho-specific antibody.

(A) Detection of Beclin 1 S90 phosphorylation by radioimmunolabeling and autoradiography (upper gel) or by western blot analysis using an anti-Beclin 1 S90 phospho-specific antibody (lower gel) in cells transfected with wild-type Flag-Beclin 1 but not the mutant Flag-Beclin 1 S90A. Starvation (-) refers to growth in normal medium and starvation (+) refers to growth in HBSS for 2 h. (B) Detection of endogenous Beclin 1 S90 phosphorylation by immunoprecipitation and immunoblot analysis and detection of autophagy by p62 and LC3 immunoblot analysis in HeLa cells at indicated time points after starvation in HBSS. Actin is shown as a loading control. For A-B, similar results were observed in three independent experiments.

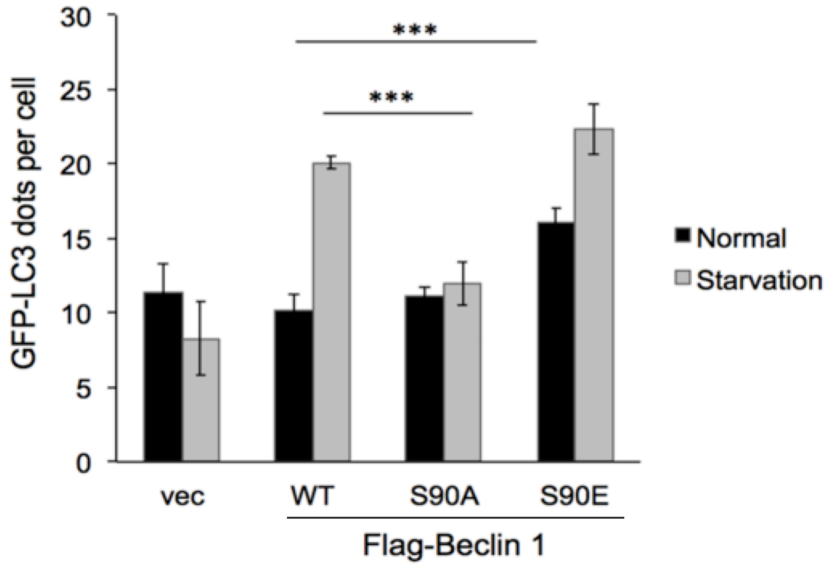

Figure 4. 3. Beclin 1 S90 phosphorylation is required for autophagy induction in MCF7 cells.

Quantification of GFP-LC3 puncta (autophagosomes) in MCF7 cells transiently co-transfected with vector (vec) or indicated Flag-Beclin 1 constructs and a plasmid expressing GFP-LC3 and grown in normal medium (starvation -) or in EBSS for 4 h (starvation +). Results represent mean $\pm$ SEM of triplicate samples ($\geq$50 cells analyzed per sample). Similar results were observed in 3 independent experiments. *** $p<0.001$. Statistics: one-way ANOVA.

A

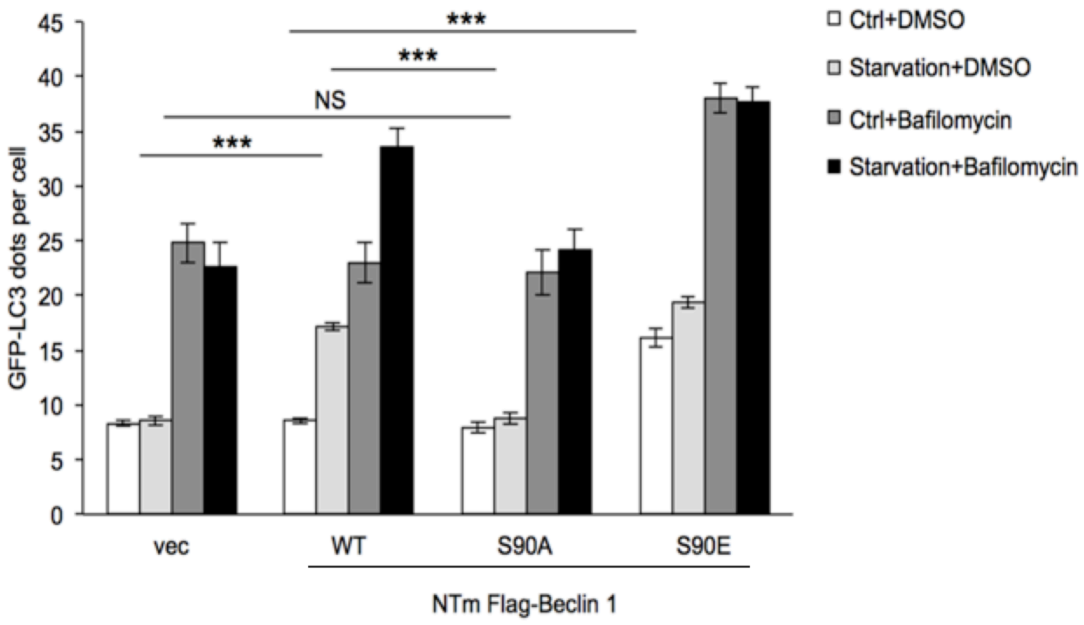

B

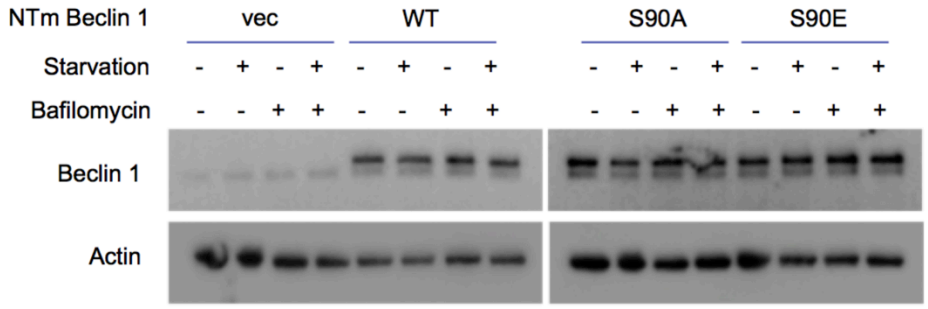

Figure 4. 4. Beclin 1 S90 phosphorylation is required for autophagy induction in *beclin 1* shRNA U2OS cells.

(A) Quantification of GFP-LC3 puncta (autophagosomes) in *beclin 1* shRNA U2OS cells (treated with 1 μg/ml doxycycline for 4 days) transiently co-transfected with vector (vec) or indicated Flag-Beclin 1 constructs and a plasmid expressing GFP-LC3 and grown in normal medium (Ctrl, control) or in EBSS for 3 h (Starvation) in the presence or absence of 100nM bafilomycin A1. Results represent mean ± SEM of triplicate samples (≥50 cells analyzed per sample). *** $p<0.001$, NS, not significant. (B) Beclin 1 expression levels in samples in (A).

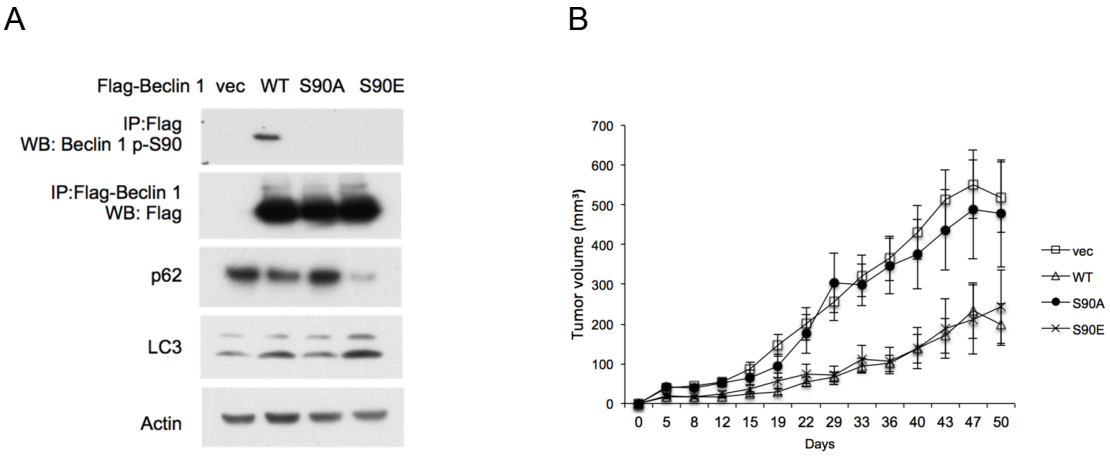

Figure 4. 5. The Beclin 1 S90 phosphorylation site is required for the tumor suppression function of Beclin 1.

(A) MCF7 cells stably expressing Flag-Beclin 1 constructs were lysed and probed with indicated antibodies. (B) Xenograft study in *nu*/*nu* mice with the same cell lines as in (A). $5x10^6$ cells were injected in the intramammary fat pad of each mouse. In each group, at least 11 mice were injected.

A

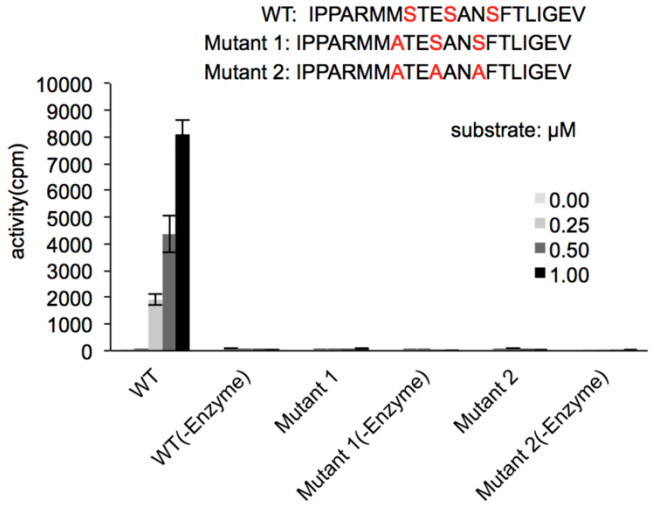

B

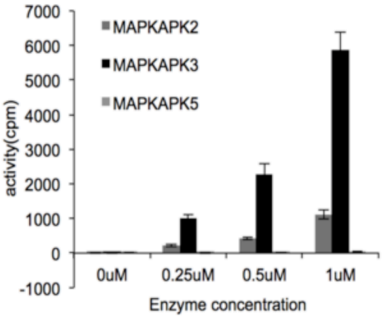

C

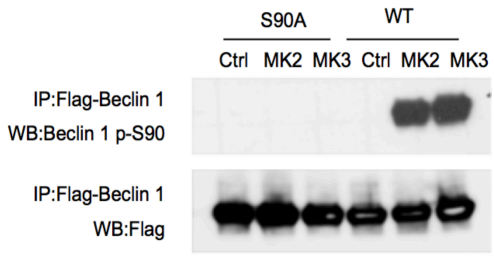

Figure 4. 6. MK2 and MK3 phosphorylate Beclin 1 S90 *in vitro.*

(A) *In vitro* kinase activity of MK2 using indicated Beclin 1 peptides as a substrate. (B) *In vitro* kinase activity of MK2, MK3, and MK5 using the wild-type (WT) Beclin 1 peptide shown in A as a substrate. (C) *In vitro* kinase activity of MK2 and MK3 using wild-type Flag-Beclin 1 or Flag-Beclin 1 S90 purified from HEK293 cells as a substrate.

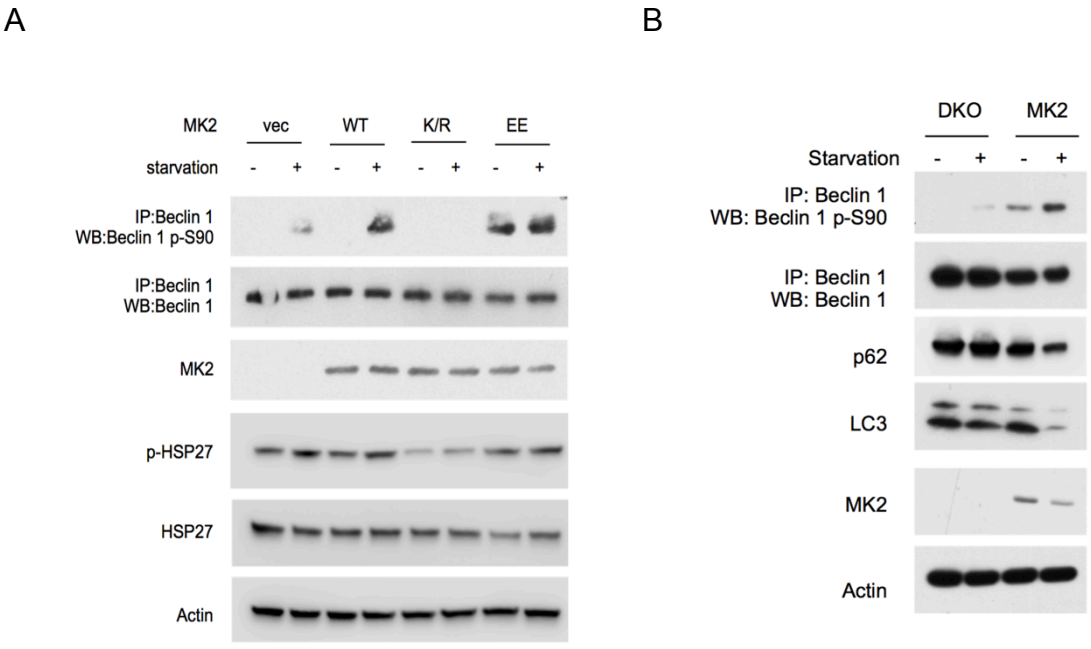

Figure 4. 7. MK2 phosphorylates Beclin 1 S90 in cultured cells.

(A) Effects of wild-type, dominant negative (K/R) and constitutively active (EE) MK2 on endogenous Beclin 1 S90 phosphorylation in HeLa cells grown in normal medium (starvation -) or HSBB for 2 h (starvation +). Phosphorylation of Hsp27 was probed to measure the activity of MK2. (B) Endogenous Beclin 1 S90 phosphorylation in MK2/3 double-knockout MEFs or MK2/3 double-knockout MEFs reconstituted with wild-type MK2. Cells were grown in normal medium (starvation -) or HBSS for 2 h (starvation +).

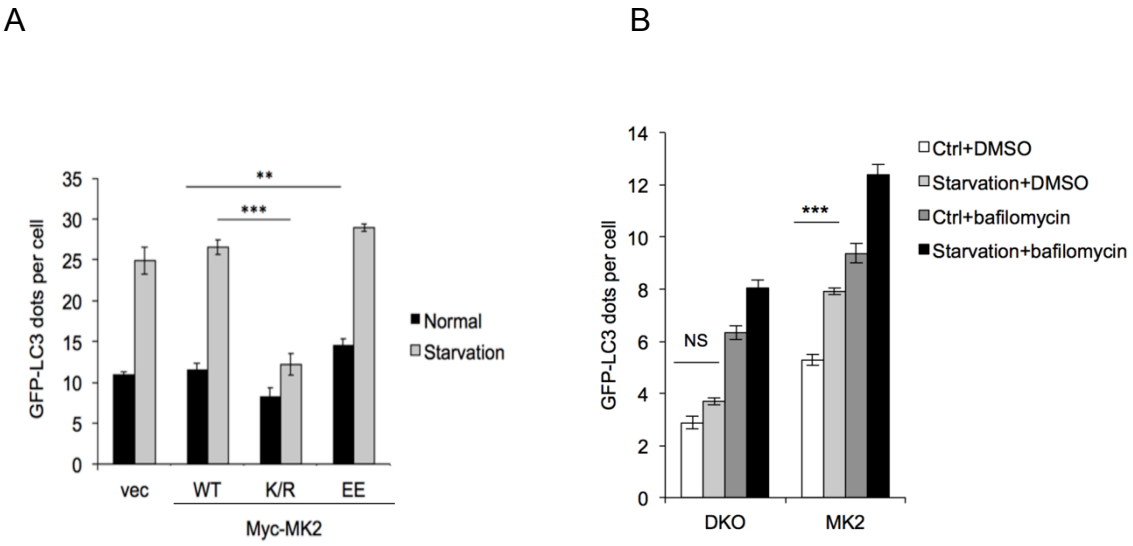

Figure 4. 8. MK2 and MK3 positively regulate autophagy.

(A) Quantification of GFP-LC3 puncta (autophagosomes) in HeLa/GFP-LC3 cells transfected with vector (vec)/indicated MK2 expression plasmid and grown in normal medium (normal) or in HBSS for 4 h (starvation). Results represent mean $\pm$ SEM of triplicate samples ($\geq$50 cells analyzed per sample). Similar results were observed in 3 independent experiments. (B) Quantification of GFP-LC3 puncta (autophagosomes) in MK2/MK3 knockout MEFs with or without stable MK2 overexpression during growth in normal medium (normal) or HBSS (starvation) for 4 h in the presence or absence of 100 nM bafilomycin A1. Results represent mean $\pm$ SEM of triplicate samples ($\geq$50 cells analyzed per sample). Similar results were observed in 3 independent experiments. ** $p<0.01$, ***$p<0.001$, NS, not significant. Statistics: one-way ANOVA.

A

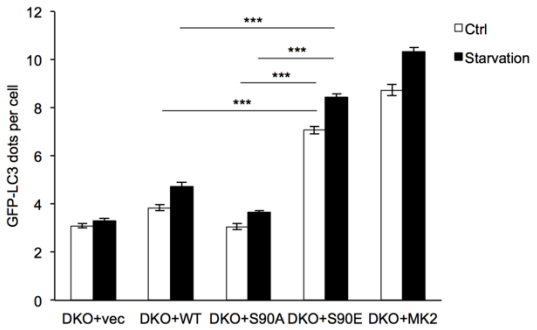

B

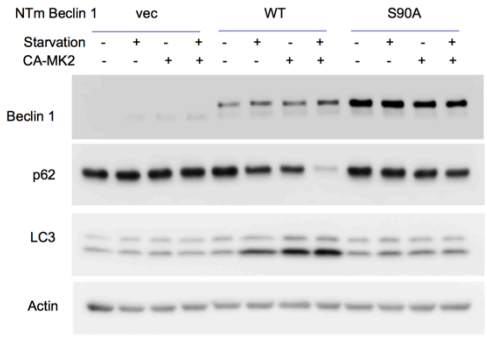

Figure 4. 9. MK2 positively regulates autophagy via Beclin 1 S90 phosphorylation.

(A) Quantification of GFP-LC3 puncta (autophagosomes) in MK2/MK3 knockout MEFs stably expressing indicated expression constructs and grown in normal medium (normal) or HBSS (starvation) for 4 h. Results represent mean ± SEM of triplicate samples (≥50 cells analyzed per sample). (B) Effects of constitutively active MK2 on autophagy (as measured by p62 and LC3 western blot analysis) in U20S doxycycline-inducible *beclin 1* shRNA knockdown cells expressing either shRNA-resistant wild-type Flag-Beclin 1 or mutant Flag-Beclin 1 S90A. Cells were treated with 1 μg/ml doxycycline for 4 days prior to western blot analyses with indicated antibodies, and transfected with indicated shRNA-resistant plasmids after 2 days of doxycycline treatment. *** $p<0.01$. Statistics: one-way ANOVA.

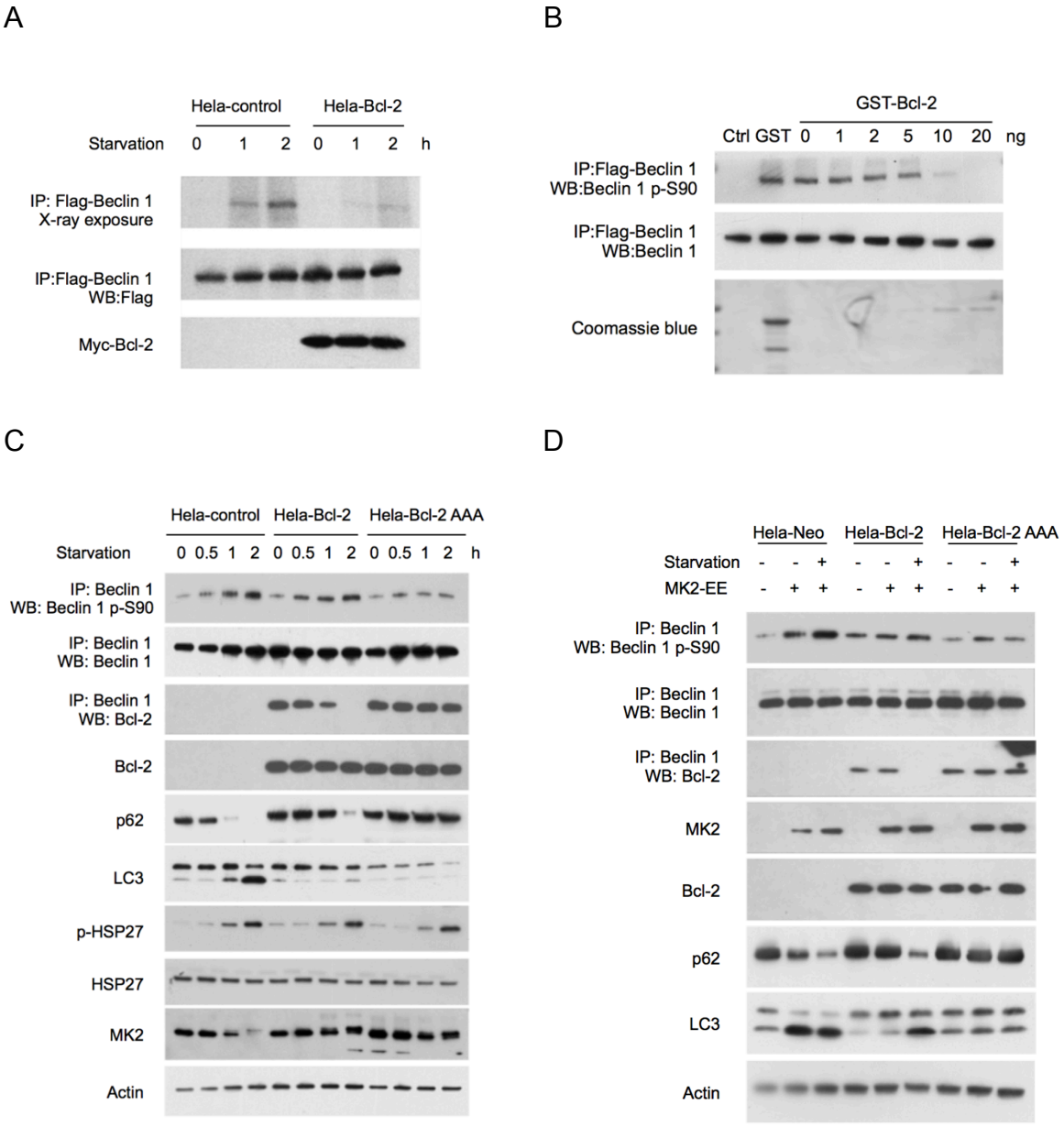

Figure 4. 10. Bcl-2 negatively regulates Beclin 1 S90 phosphorylation.

(A) HeLa cells stably expressing the control vector (HeLa-control) or Bcl-2 were transiently transfected with Flag-Beclin 1 and starved with HBSS for indicated duration. Phosphorylated Flag-Beclin 1 was labeled with P^{32} and visualized by X-ray exposure. (B) *In vitro* kinase activity of MK2 using Flag-Beclin 1 purified from HEK293 cells as a substrate in the presence of the indicated amount of GST-Bcl-2. (C) Detection of Beclin 1 S90 phosphorylation and autophagy levels (as measured by p62 and LC3 immunoblots) in HeLa cells stably transfected with empty vector, wild-type Bcl-2, or a Bcl-2 AAA mutant and

subjected to starvation in HBSS for the indicated time period. p-Hsp27 protein levels are shown as an indicator of MK2 activation. (D) Detection of Beclin 1 S90 phosphorylation and autophagy levels (as measured by p62 and LC3 immunoblots) in HeLa cells stably transfected with empty vector, wild-type Bcl-2, or a Bcl-2 AAA mutant and transiently transfected with a control empty vector or constitutively active MK2 (MK2 EE) and grown in normal medium (starvation -) or HBSS for 2 h (starvation +).

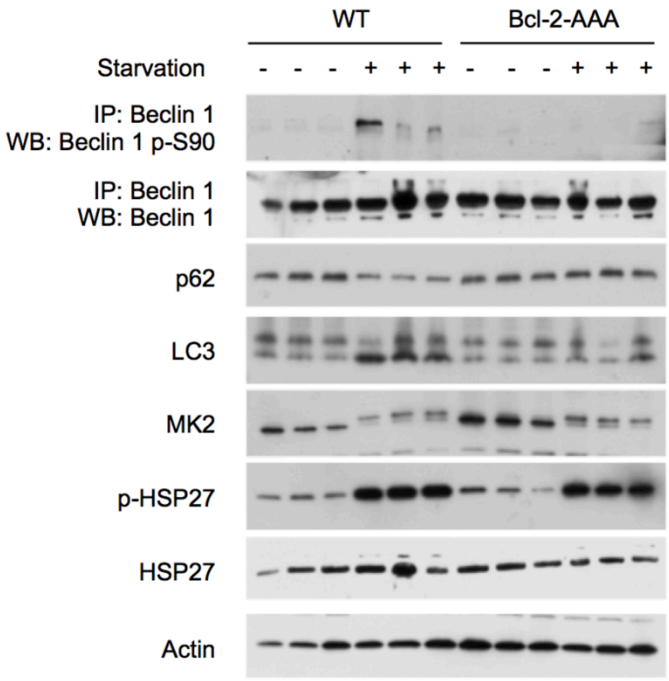

Figure 4. 11. Bcl-2 negatively regulates starvation-induced Beclin 1 S90 phosphorylation *in vivo*.

Defective starvation-induced Beclin 1 S90 phosphorylation and autophagy induction in vastus lateralis muscle of Bcl-2 AAA mice. Wild-type and Bcl-2 AAA mice were subjected to starvation for 48 h prior to tissue collection, and western blot analysis of muscle lysates with indicated antibodies.

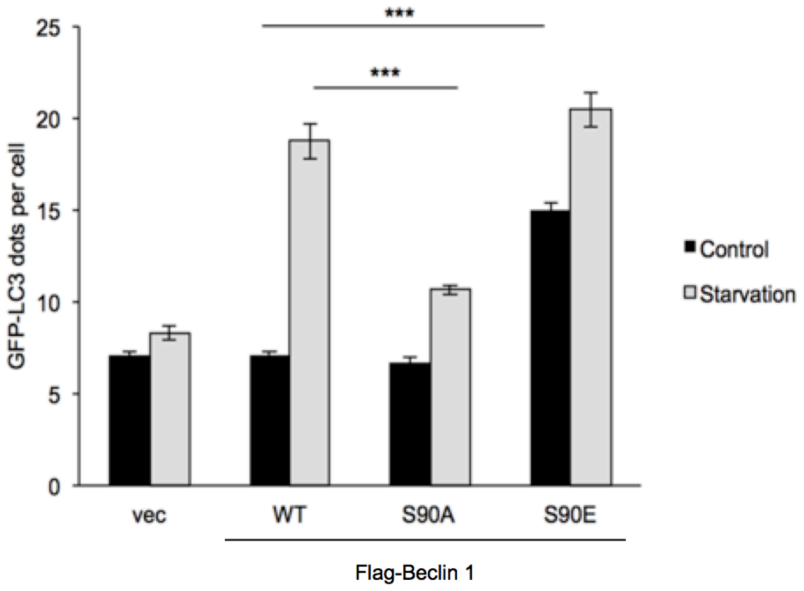

Figure 4. 12. Beclin 1 S90E is sufficient to induce autophagy in Bcl-2 AAA MEFs.

Reversal of the block in starvation-induced autophagy (as measured by quantification of GFP-LC3 puncta in normal medium and 4 h after HBSS starvation) by overexpression of vector (vec)/wild-type Flag-Beclin 1 and Flag-Beclin 1 S90E, but not of Flag-Beclin 1 S90A, in primary Bcl-2 AAA MEFs. MEFs were co-transfected with GFP-LC3 and indicated Beclin 1 expression plasmid. Results represent mean $\pm$ SEM of triplicate samples ($\geq$50 cells analyzed per sample). Similar results were observed in 3 independent experiments. *** $p<0.001$. Statistics: one-way ANOVA.

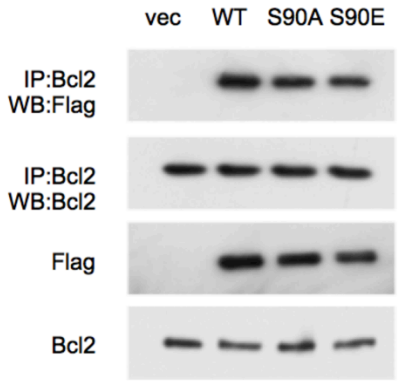

Figure 4. 13. Beclin 1 S90 phosphorylation does not facilitate Bcl-2 dissociation.

Beclin 1/Bcl-2 binding in U2OS doxycycline-inducible *beclin 1* shRNA knockdown cells expressing either shRNA-resistant wild-type Flag-Beclin 1, mutant Flag-Beclin 1 S90A, or mutant Flag-Beclin 1 S90E. Cells were treated with 1 μg/ml doxycycline for 4 days prior to western blot analyses with indicated antibodies, and transfected with indicated shRNA-resistant plasmids after 2 days of doxycycline treatment.

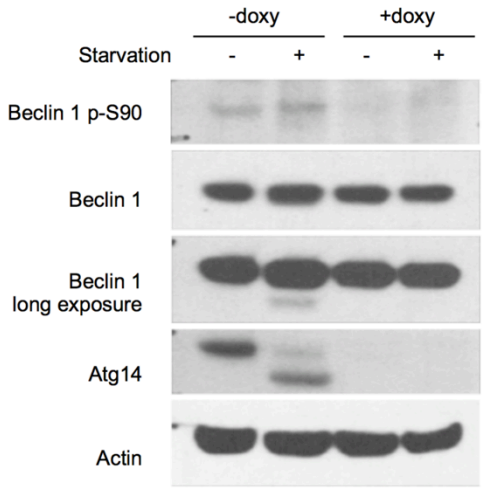

Figure 4. 14. Atg14 is essential for Beclin 1 S90 phosphorylation.

The effect of Atg14 on Beclin 1 S90 phosphorylation was examined in U2OS doxycycline-inducible *ATG14* shRNA knockdown cells. Cells were treated with 1 μg/ml doxycycline for 3 days prior to western blot analyses with indicated antibodies.

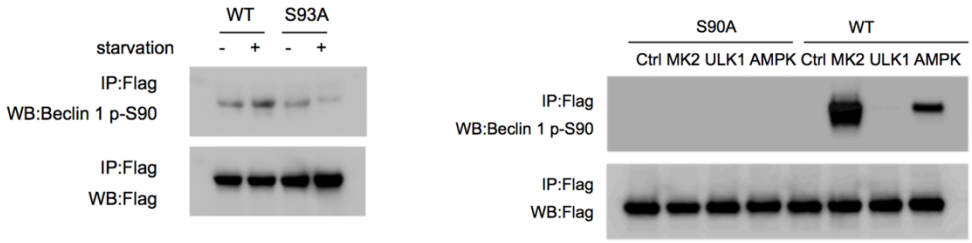

Figure 4. 15. Beclin 1 S93 phosphorylation and AMPK may regulate Beclin 1 S90 phosphorylation.

(A) HeLa cells were transfected with wild-type Flag-Beclin 1 or Flag-Beclin 1 S93A and grown in normal (starvation -) or HBSS (starvation +) for 2 h. (B) *In vitro* kinase activity of MK2, Ulk1 and AMPK using wild-type Flag-Beclin 1 or Flag-Beclin 1 S90A purified from HEK293 cells as a substrate.

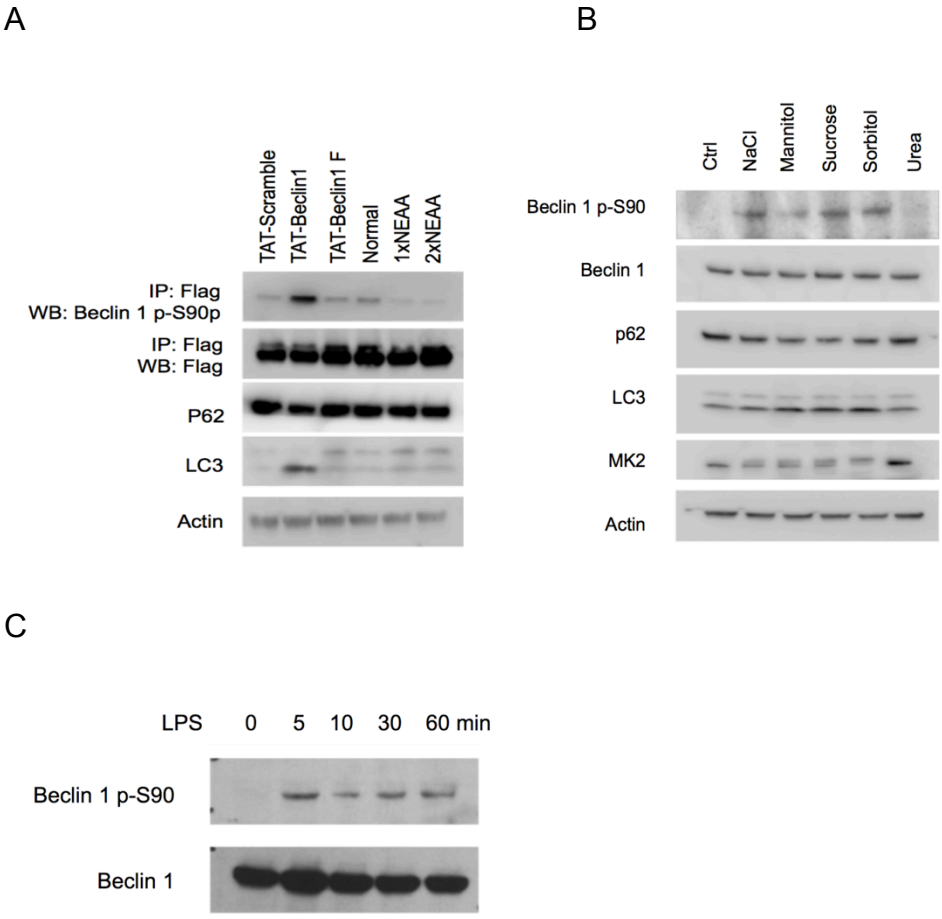

Figure 4. 16. Beclin 1 S90 phosphorylation is regulated by multiple stimuli.

(A) Beclin 1 S90 phosphorylation is induced by an autophagy-inducing peptide (Tat-Beclin 1) but not by point mutant (Tat-Beclin 1 F270S) or scrambled control mutant (Tat-Scrambled) peptides that do not induce autophagy in SKNSH-Flag-Beclin 1 cells. Excess levels of amino acids (i.e. culturing cells with 1x or 2x non-essential amino acids (NEAA)) decrease Beclin 1 S90 phosphorylation. Similar results were observed in three independent experiments. (peptide concentration: 30 μM, 3h treatment) (B) Osmotic stress induces Beclin 1 S90 phosphorylation and autophagy. HeLa cells were treated with additional 150 mM NaCl, 300 mM mannitol, 300 mM sucrose, 300 mM sorbitol or 300 mM urea for 10 min and cell lysates were used in western blotting using indicated antibodies. (C) 1 μg/mL LPS induces Beclin 1 S90 phosphorylation in primary bone marrow-derived macrophages.

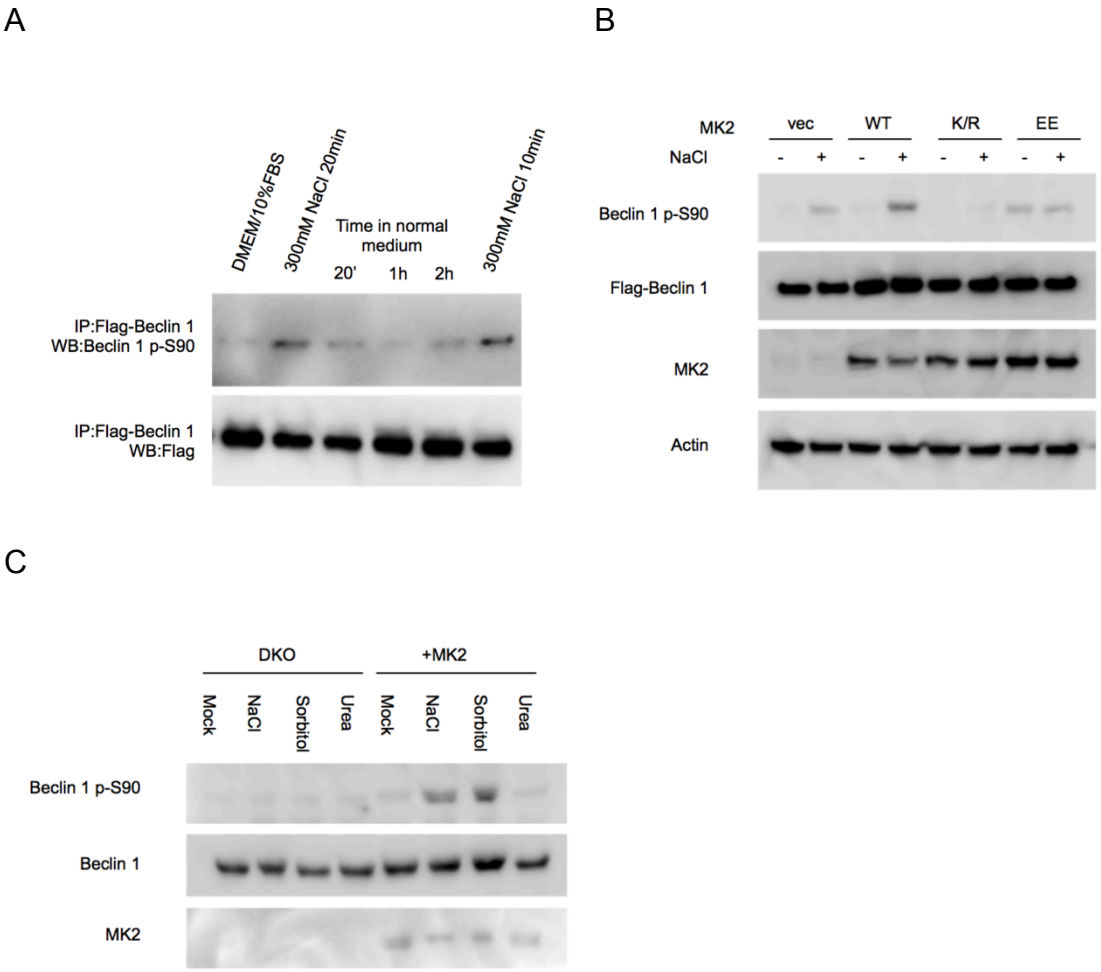

Figure 4. 17. MK2/3-mediated Beclin 1 S90 phosphorylation is induced by osmotic stress.

(A) Osmotic stress induces Beclin 1 S90 phosphorylation in HeLa cells. (B) Effects of wild-type, dominant negative (K/R) and constitutively active (EE) MK2 on endogenous Beclin 1 S90 phosphorylation in HeLa cells grown in normal medium (NaCl -) or medium with high osmotic stress (NaCl +) for 20 min. (C) Endogenous Beclin 1 S90 phosphorylation in MK2/3 double-knockout MEFs or MK2/3 double-knockout MEFs reconstituted with wild-type MK2. Cells were grown in in normal medium or medium with 300mM NaCl, 300mM sorbitol or 300 mM urea for 20 min.

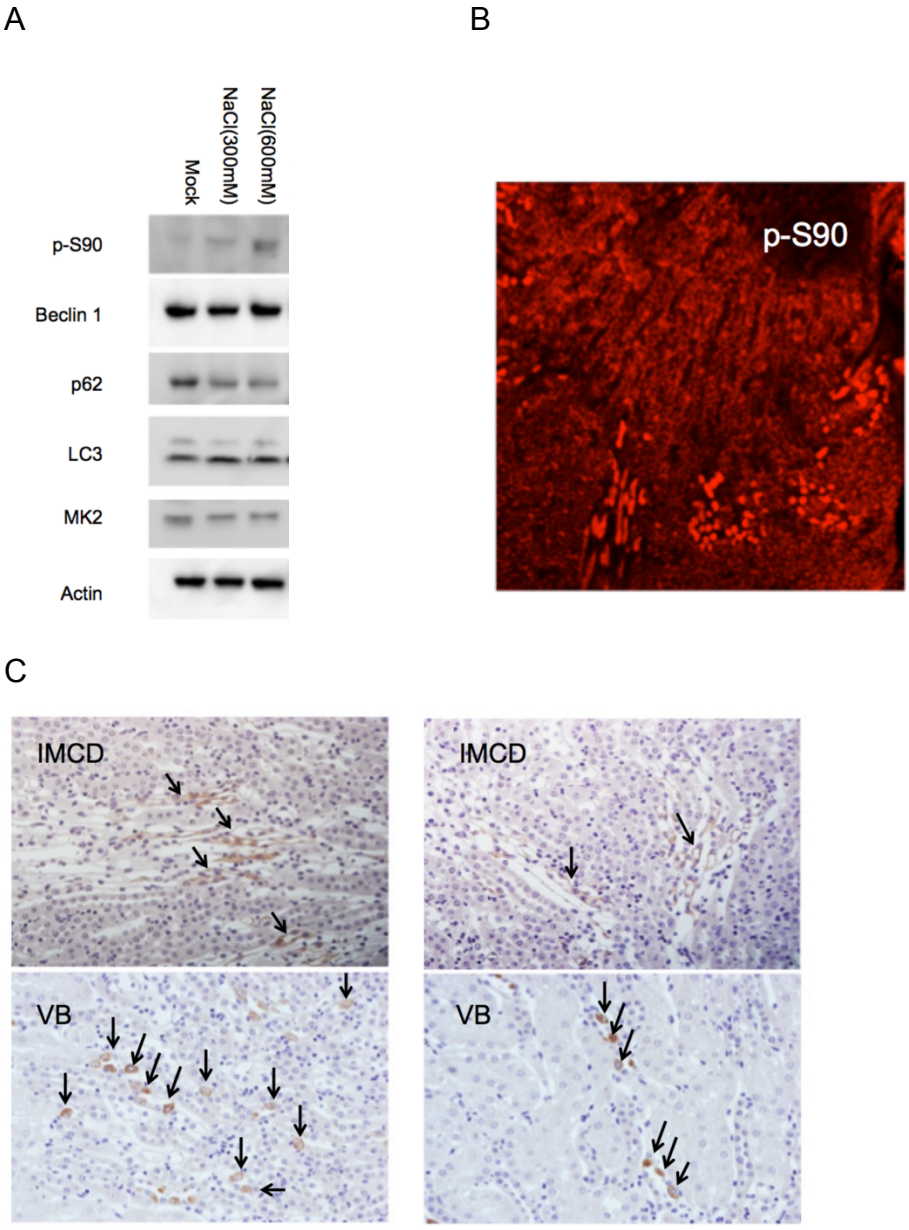

Figure 4. 18. Beclin 1 S90 phosphorylation is induced by osmotic stress *in vivo*.

(A) Osmotic stress induces Beclin 1 S90 phosphorylation in mouse inner medullary connecting duct cells (mIMCD3 cells). (B) Immunofluorescent staining of the mouse kidney section with the Beclin 1 p-S90 antibody. (C) Immunostaining of the mouse kidney section with the Beclin 1 p-S90 antibody. IMCD, inner medullary collecting duct. VB, vascular bundle.

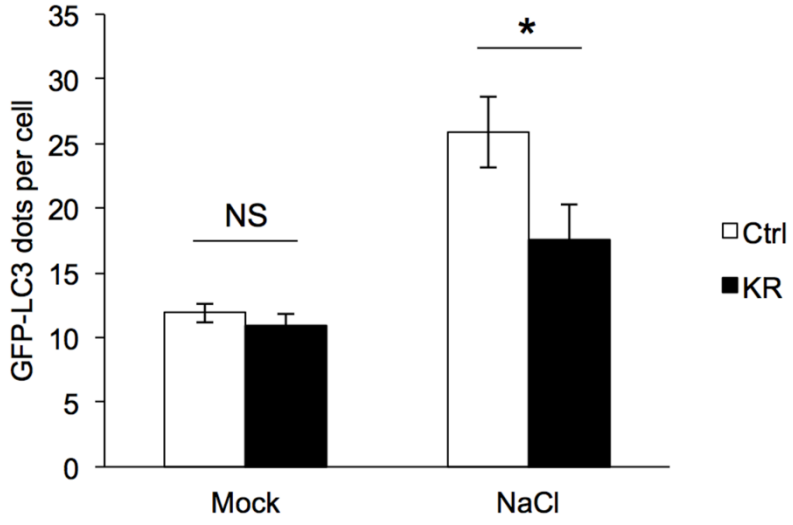

Figure 4. 19 Dominant-negative MK2 decreases high osmotic stress-induced autophagy.

Quantification of GFP-LC3 puncta (autophagosomes) in HeLa/GFP-LC3 cells transfected with indicated MK2 expression plasmid and grown in normal medium (Mock) or in 300 mM NaCl containing medium for 30 min (NaCl). Results represent mean $\pm$ SEM of triplicate samples ($\geq$50 cells analyzed per sample). Similar results were observed in 3 independent experiments. * $p<0.05$, NS, not significant. Statistics: one-way ANOVA.

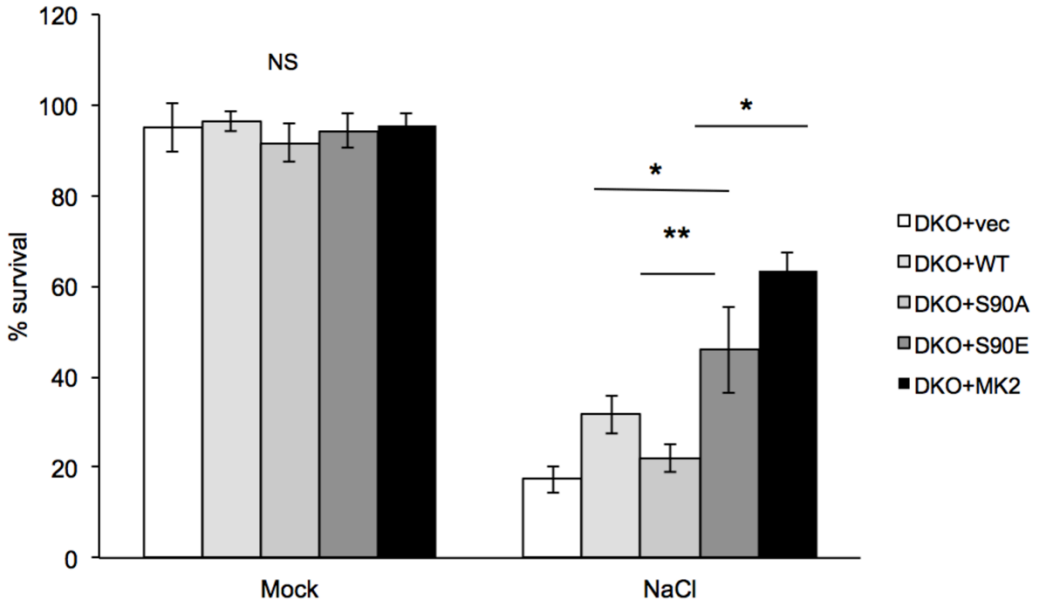

Figure 4. 20 Beclin 1 S90 phosphorylation is essential for cell survival under high osmotic stress.

Survived cells in MK2/MK3 knockout MEFs stably expressing indicated expression constructs and grown in normal medium (Mock) or 300mM NaCl for 8h were quantified by trypan blue assay. * $p<0.05$, ** $p<0.01$, NS, not significant. Statistics: one-way ANOVA.

CHAPTER FIVE

Conclusions and Future directions

I. Conclusions

The role of autophagy in regulating different physiological processes continues to expand. The complicated regulation of autophagy by different signaling pathways under different conditions is also under comprehensive study. The aims of our studies are to explore the regulatory role of autophagy in quiescence entry and also the regulation of starvation and osmotic stress-induced autophagy by Beclin 1 phosphorylation. The most important findings from the present study are listed below:

For the quiescence study, we found that:

1. *Saccharomyces cerevisiae* with null mutations in essential autophagy genes (*ATG1*, *ATG5*, *VPS30*/*ATG6*, *ATG7*, and *ATG8*) fail to arrest in G_1/G_0 after nitrogen and carbon starvation.

2. *Saccharomyces cerevisiae* with null mutations in essential autophagy genes arrest in telophase after nitrogen starvation.

3. Autophagy null yeasts display quiescent-specific phenotypes such as activation of Snf1, resistance to heat shock and accumulation of glycogen and trehalose accumulation after nitrogen starvation.

4. Vacuolar proteases, but not vacuolar permeases, are required for proper G_1/G_0 entry.

For the Beclin 1 phosphorylation study, we found that:

1. Beclin 1 S90 is phosphorylated in response to stimuli such as starvation, osmotic stress and LPS treatment. This phosphorylation is essential for autophagy induction and is required for the tumor suppressor activity of Beclin 1.

2. MK2/MK3 are kinases newly identified to be involved in the regulation of autophagy.

3. MK2/MK3 phosphorylate Beclin 1 both *in vitro* and *in vivo* on amino acid residue serine 90

4. MK2/3 positively regulate autophagy by phosphorylating Beclin 1 S90.

5. The interaction between Bcl-2 and Beclin 1 inhibits Beclin 1 S90 phosphorylation and autophagy.

6. Atg14 is required for Beclin 1 S90 phosphorylation. AMPK positively regulate Beclin 1 S90 phosphorylation.

7. Beclin 1 S90 phosphorylation is present in the regions of mouse kidney where osmolality is high. Beclin 1 S90 phosphorylation is important for cell survival under high osmotic stress.

8. Beclin 1 S90 phosphorylation is diminished in the presence of a mutation in Beclin 1 S93.

II. Future directions

1. Future directions for the yeast cell cycle arrest project

Our current data, together with the findings from other groups indicate that autophagy is critical for proper G_1/G_0 cell cycle arrest during nitrogen starvation (Matsui et al., 2013). However, the precise mechanisms by which autophagy regulates G_1/G_0 cell cycle arrest still

need to be elucidated. Our results showed an interesting observation that autophagy-deficient yeasts exhibit deficiency in cell cycle progression only under starvation, but not under nutrient rich conditions. More interestingly, *pep4*Δ yeasts, which cannot produce mature lysosomal enzymes are deficient in cell cycle progression under both nutrient rich and starvation conditions, indicating that the lysosomal degradation machinery is very important in cell cycle regulation.

The lysosomal degradation machinery may function in two ways to regulate the cell cycle:

1. Degradation of cell cycle regulators

One important function of autophagy is to degrade cytoplasmic contents. Therefore, it is reasonable to speculate that degradation of certain cell cycle regulators is blocked in *ATG* deficient yeasts. We found that after nitrogen starvation, *ATG* deficient yeasts arrested in telophase and failed to exit mitosis. There are some candidate proteins regulating mitotic exit such as Clb2, Pds1 and Cut2 (King et al., 1996). Although it was reported that those proteins are degraded through the proteasome pathway (King et al., 1996), it will be interesting to know if these proteins are degraded via the autophagic pathway under certain conditions such as starvation.

2. Providing nutrients upon starvation

Another key role of autophagy is to maintain energy homeostasis under stress. Therefore we speculated if nutrient recycling is critical for proper G_1/G_0 cell cycle arrest. Interestingly, we

found that *avt3*Δ*avt4*Δ*atg22*Δ yeasts deficient in nutrient recycling arrested in G_1/G_0 after nitrogen starvation. One possibility is that there may be other unreported vacuole permeases functioning redundantly. Another possibility is that nutrient recycling is not required for proper G_1/G_0 cell cycle arrest after starvation. Further experiments are required to give a clear answer to this question.

Another interesting point is that in response to glucose starvation, we also observed a deficiency in G_1/G_0 cell cycle arrest in autophagy-deficient yeasts. It will be interesting to know if similar findings can be observed under other autophagy-inducing conditions. Further analyses of G_1/G_0 cell cycle arrest in response to glucose starvation and other stressors may help us further understand the regulatory mechanism by which autophagy regulates proper G_1/G_0 quiescence.

2. Future directions for the Beclin 1 phosphorylation project

In this project, we identified a phosphorylation site of Beclin 1 essential for autophagy induction after starvation. The phosphorylation is mediated by MK2/3 and positively regulated by Atg14 and AMPK. Interestingly, Bcl-2 binding blocks Beclin 1 S90 phosphorylation, which provides a potential mechanism by which Bcl-2 blocks autophagy. We also found that osmotic stress is a potent inducer of Beclin 1 S90 phosphorylation and that S90 phosphorylation is important for cell survival under osmotic stress. The construction of Beclin 1 S90A and S90E knock-in mice will be very helpful to further understand the physiological functions of Beclin 1 S90 phosphorylation *in vivo*.

In the proximity of Beclin 1 S90, there are two other serine residues, S93 and S96, which can be phosphorylated by AMPK in response to glucose starvation (Kim et al., 2013). Interestingly, we found that amino acid starvation-induced S90 phosphorylation is diminished when S93 is mutated to alanine. However, we did not test if phosphorylation of S96 regulates S90 phosphorylation. It is also not clear if AMPK phosphorylates S93 and S96 after nitrogen starvation (A personal communication from Dr. Kun-Liang Guan at UCSD indicates that it does not). There is also another amino acid T91 next to S90, which can also potentially regulate S90 phosphorylation. Investigations of whether amino acid starvation induces the phosphorylation of T91, S93 and S96 and of the interplay among these phosphorylation events are of potential interest.

Atg14 was identified as an essential protein for Beclin 1 S90 phosphorylation (Fogel et al., 2013). It was reported that the Beclin 1-PI3K complex associate with Atg14 and Rubicon, separately. While Atg14 enhances lipid kinase activity of Vps34 and upregulates autophagy, Rubicon reduces Vps34 activity and represses autophagy. By interacting with different regulators, the Beclin 1-PI3K complex coordinates autophagy levels. It is possible that only Atg14-associated Beclin 1 is phosphorylated on S90. This hypothesis could be tested in the future by immunoprecipitating Atg14 and other Beclin 1-binding partners and examining the levels of Beclin 1 S90 phosphorylation in the different immunoprecipitates. Moreover, whether Beclin 1 S90 phosphorylation changes its binding partners or subcellular localization is not clear. Additional experiments need to be performed to investigate these questions.

Starvation and osmotic stress-induced Beclin 1 S90 phosphorylation was mediated by MK2/3 as shown in this study. Additionally, UV, LPS, reactive oxygen species and some drugs are also activators of MK2/3 (Gaestel, 2006). It will be interesting to determine if these stressors also induce Beclin 1 S90 phosphorylation and if Beclin 1 S90 phosphorylation acts as a protective mechanism against cell death under such stress conditions.

References

Abeliovich, H., and Klionsky, D.J. (2001). Autophagy in yeast: mechanistic insights and physiological function. Microbiology and molecular biology reviews : MMBR *65*, 463-479, table of contents.

Bellot, G., Garcia-Medina, R., Gounon, P., Chiche, J., Roux, D., Pouyssegur, J., and Mazure, N.M. (2009). Hypoxia-induced autophagy is mediated through hypoxia-inducible factor induction of BNIP3 and BNIP3L via their BH3 domains. Molecular and cellular biology *29*, 2570-2581.

Betz, C., and Hall, M.N. (2013). Where is mTOR and what is it doing there? The Journal of cell biology *203*, 563-574.

Cargnello, M., and Roux, P.P. (2011). Activation and function of the MAPKs and their substrates, the MAPK-activated protein kinases. Microbiology and molecular biology reviews : MMBR *75*, 50-83.

Chen, Y., and Klionsky, D.J. (2011). The regulation of autophagy - unanswered questions. Journal of cell science *124*, 161-170.

Cherra, S.J., 3rd, Kulich, S.M., Uechi, G., Balasubramani, M., Mountzouris, J., Day, B.W., and Chu, C.T. (2010). Regulation of the autophagy protein LC3 by phosphorylation. The Journal of cell biology *190*, 533-539.

Clifton, A.D., Young, P.R., and Cohen, P. (1996). A comparison of the substrate specificity of MAPKAP kinase-2 and MAPKAP kinase-3 and their activation by cytokines and cellular stress. FEBS letters *392*, 209-214.

Cloonan, S.M., and Williams, D.C. (2011). The antidepressants maprotiline and fluoxetine induce Type II autophagic cell death in drug-resistant Burkitt's lymphoma. International journal of cancer Journal international du cancer *128*, 1712-1723.

Daignan-Fornier, B., and Sagot, I. (2011). Proliferation/Quiescence: When to start? Where to stop? What to stock? Cell division *6*, 20.

Efeyan, A., Zoncu, R., and Sabatini, D.M. (2012). Amino acids and mTORC1: from lysosomes to disease. Trends in molecular medicine *18*, 524-533.

Feng, Y., He, D., Yao, Z., and Klionsky, D.J. (2014). The machinery of macroautophagy. Cell research *24*, 24-41.

Fimia, G.M., Stoykova, A., Romagnoli, A., Giunta, L., Di Bartolomeo, S., Nardacci, R., Corazzari, M., Fuoco, C., Ucar, A., Schwartz, P.*, et al.* (2007). Ambra1 regulates autophagy and development of the nervous system. Nature *447*, 1121-1125.

Fogel, A.I., Dlouhy, B.J., Wang, C., Ryu, S.W., Neutzner, A., Hasson, S.A., Sideris, D.P., Abeliovich, H., and Youle, R.J. (2013). Role of membrane association and Atg14-dependent phosphorylation in beclin-1-mediated autophagy. Molecular and cellular biology *33*, 3675-3688.

Gaestel, M. (2006). MAPKAP kinases - MKs - two's company, three's a crowd. Nature reviews Molecular cell biology *7*, 120-130.

George, M.D., Baba, M., Scott, S.V., Mizushima, N., Garrison, B.S., Ohsumi, Y., and Klionsky, D.J. (2000). Apg5p functions in the sequestration step in the cytoplasm-to-vacuole targeting and macroautophagy pathways. Molecular biology of the cell *11*, 969-982.

Gerhardt, B., Kordas, T.J., Thompson, C.M., Patel, P., and Vida, T. (1998). The vesicle transport protein Vps33p is an ATP-binding protein that localizes to the cytosol in an energy-dependent manner. The Journal of biological chemistry *273*, 15818-15829.

Glick, D., Barth, S., and Macleod, K.F. (2010). Autophagy: cellular and molecular mechanisms. The Journal of pathology *221*, 3-12.

Gray, J.V., Petsko, G.A., Johnston, G.C., Ringe, D., Singer, R.A., and Werner-Washburne, M. (2004). "Sleeping beauty": quiescence in Saccharomyces cerevisiae. Microbiology and molecular biology reviews : MMBR *68*, 187-206.

Green, D.R., and Levine, B. (2014). To be or not to be? How selective autophagy and cell death govern cell fate. Cell *157*, 65-75.

Hancioglu, B., and Tyson, J.J. (2012). A mathematical model of mitotic exit in budding yeast: the role of Polo kinase. PloS one *7*, e30810.

He, C., Bassik, M.C., Moresi, V., Sun, K., Wei, Y., Zou, Z., An, Z., Loh, J., Fisher, J., Sun, Q.*, et al.* (2012). Exercise-induced BCL2-regulated autophagy is required for muscle glucose homeostasis. Nature *481*, 511-515.

He, C., and Levine, B. (2010). The Beclin 1 interactome. Current opinion in cell biology *22*, 140-149.

Inoki, K., Kim, J., and Guan, K.L. (2012). AMPK and mTOR in cellular energy homeostasis and drug targets. Annual review of pharmacology and toxicology *52*, 381-400.

Jorgensen, P., and Tyers, M. (2004). How cells coordinate growth and division. Current biology : CB *14*, R1014-1027.

Kabeya, Y., Kamada, Y., Baba, M., Takikawa, H., Sasaki, M., and Ohsumi, Y. (2005). Atg17 functions in cooperation with Atg1 and Atg13 in yeast autophagy. Molecular biology of the cell *16*, 2544-2553.

Kang, R., Zeh, H.J., Lotze, M.T., and Tang, D. (2011). The Beclin 1 network regulates autophagy and apoptosis. Cell death and differentiation *18*, 571-580.

Kanki, T., Wang, K., Cao, Y., Baba, M., and Klionsky, D.J. (2009). Atg32 is a mitochondrial protein that confers selectivity during mitophagy. Developmental cell *17*, 98-109.

Kim, J., Dalton, V.M., Eggerton, K.P., Scott, S.V., and Klionsky, D.J. (1999). Apg7p/Cvt2p is required for the cytoplasm-to-vacuole targeting, macroautophagy, and peroxisome degradation pathways. Molecular biology of the cell *10*, 1337-1351.

Kim, J., Huang, W.P., and Klionsky, D.J. (2001a). Membrane recruitment of Aut7p in the autophagy and cytoplasm to vacuole targeting pathways requires Aut1p, Aut2p, and the autophagy conjugation complex. The Journal of cell biology *152*, 51-64.

Kim, J., Kamada, Y., Stromhaug, P.E., Guan, J., Hefner-Gravink, A., Baba, M., Scott, S.V., Ohsumi, Y., Dunn, W.A., Jr., and Klionsky, D.J. (2001b). Cvt9/Gsa9 functions in sequestering selective cytosolic cargo destined for the vacuole. The Journal of cell biology *153*, 381-396.

Kim, J., Kim, Y.C., Fang, C., Russell, R.C., Kim, J.H., Fan, W., Liu, R., Zhong, Q., and Guan, K.L. (2013). Differential regulation of distinct Vps34 complexes by AMPK in nutrient stress and autophagy. Cell *152*, 290-303.

Kim, J., Kundu, M., Viollet, B., and Guan, K.L. (2011). AMPK and mTOR regulate autophagy through direct phosphorylation of Ulk1. Nature cell biology *13*, 132-141.

King, R.W., Deshaies, R.J., Peters, J.M., and Kirschner, M.W. (1996). How proteolysis drives the cell cycle. Science *274*, 1652-1659.

Kirisako, T., Ichimura, Y., Okada, H., Kabeya, Y., Mizushima, N., Yoshimori, T., Ohsumi, M., Takao, T., Noda, T., and Ohsumi, Y. (2000). The reversible modification regulates the membrane-binding state of Apg8/Aut7 essential for autophagy and the cytoplasm to vacuole targeting pathway. The Journal of cell biology *151*, 263-276.

Kroemer, G., and Levine, B. (2008). Autophagic cell death: the story of a misnomer. Nature reviews Molecular cell biology *9*, 1004-1010.

Kroemer, G., Marino, G., and Levine, B. (2010). Autophagy and the integrated stress response. Molecular cell *40*, 280-293.

Laporte, D., Lebaudy, A., Sahin, A., Pinson, B., Ceschin, J., Daignan-Fornier, B., and Sagot, I. (2011). Metabolic status rather than cell cycle signals control quiescence entry and exit. The Journal of cell biology *192*, 949-957.

Lee, I.H., Cao, L., Mostoslavsky, R., Lombard, D.B., Liu, J., Bruns, N.E., Tsokos, M., Alt, F.W., and Finkel, T. (2008). A role for the NAD-dependent deacetylase Sirt1 in the regulation of autophagy. Proceedings of the National Academy of Sciences of the United States of America *105*, 3374-3379.

Lee, I.H., and Finkel, T. (2009). Regulation of autophagy by the p300 acetyltransferase. The Journal of biological chemistry *284*, 6322-6328.

Lee, I.H., Kawai, Y., Fergusson, M.M., Rovira, II, Bishop, A.J., Motoyama, N., Cao, L., and Finkel, T. (2012). Atg7 modulates p53 activity to regulate cell cycle and survival during metabolic stress. Science *336*, 225-228.

Levine, B., and Kroemer, G. (2008). Autophagy in the pathogenesis of disease. Cell *132*, 27-42.

Liang, X.H., Jackson, S., Seaman, M., Brown, K., Kempkes, B., Hibshoosh, H., and Levine, B. (1999). Induction of autophagy and inhibition of tumorigenesis by beclin 1. Nature *402*, 672-676.

Lin, S.Y., Li, T.Y., Liu, Q., Zhang, C., Li, X., Chen, Y., Zhang, S.M., Lian, G., Liu, Q., Ruan, K.*, et al.* (2012). GSK3-TIP60-ULK1 signaling pathway links growth factor deprivation to autophagy. Science *336*, 477-481.

Matsui, A., Kamada, Y., and Matsuura, A. (2013). The role of autophagy in genome stability through suppression of abnormal mitosis under starvation. PLoS genetics *9*, e1003245.

Mazure, N.M., and Pouyssegur, J. (2010). Hypoxia-induced autophagy: cell death or cell survival? Current opinion in cell biology *22*, 177-180.

McCartney, R.R., and Schmidt, M.C. (2001). Regulation of Snf1 kinase. Activation requires phosphorylation of threonine 210 by an upstream kinase as well as a distinct step mediated by the Snf4 subunit. The Journal of biological chemistry *276*, 36460-36466.

McEwan, D.G., and Dikic, I. (2011). The Three Musketeers of Autophagy: phosphorylation, ubiquitylation and acetylation. Trends in cell biology *21*, 195-201.

Mizushima, N., Yoshimori, T., and Levine, B. (2010). Methods in mammalian autophagy research. Cell *140*, 313-326.

Neufeld, T.P. (2010). TOR-dependent control of autophagy: biting the hand that feeds. Current opinion in cell biology *22*, 157-168.

New, L., Jiang, Y., Zhao, M., Liu, K., Zhu, W., Flood, L.J., Kato, Y., Parry, G.C., and Han, J. (1998). PRAK, a novel protein kinase regulated by the p38 MAP kinase. The EMBO journal *17*, 3372-3384.

Obara, K., and Ohsumi, Y. (2011). Atg14: a key player in orchestrating autophagy. International journal of cell biology *2011*, 713435.

Oberstein, A., Jeffrey, P.D., and Shi, Y. (2007). Crystal structure of the Bcl-XL-Beclin 1 peptide complex: Beclin 1 is a novel BH3-only protein. The Journal of biological chemistry *282*, 13123-13132.

Papinski, D., Schuschnig, M., Reiter, W., Wilhelm, L., Barnes, C.A., Maiolica, A., Hansmann, I., Pfaffenwimmer, T., Kijanska, M., Stoffel, I.*, et al.* (2014). Early steps in autophagy depend on direct phosphorylation of Atg9 by the Atg1 kinase. Molecular cell *53*, 471-483.

Parrou, J.L., and Francois, J. (1997). A simplified procedure for a rapid and reliable assay of both glycogen and trehalose in whole yeast cells. Analytical biochemistry *248*, 186-188.

Pattingre, S., Tassa, A., Qu, X., Garuti, R., Liang, X.H., Mizushima, N., Packer, M., Schneider, M.D., and Levine, B. (2005). Bcl-2 antiapoptotic proteins inhibit Beclin 1-dependent autophagy. Cell *122*, 927-939.

Qu, X., Yu, J., Bhagat, G., Furuya, N., Hibshoosh, H., Troxel, A., Rosen, J., Eskelinen, E.L., Mizushima, N., Ohsumi, Y.*, et al.* (2003). Promotion of tumorigenesis by heterozygous disruption of the beclin 1 autophagy gene. The Journal of clinical investigation *112*, 1809-1820.

Robinson, J.S., Klionsky, D.J., Banta, L.M., and Emr, S.D. (1988). Protein sorting in Saccharomyces cerevisiae: isolation of mutants defective in the delivery and processing of multiple vacuolar hydrolases. Molecular and cellular biology *8*, 4936-4948.

Ronkina, N., Kotlyarov, A., Dittrich-Breiholz, O., Kracht, M., Hitti, E., Milarski, K., Askew, R., Marusic, S., Lin, L.L., Gaestel, M.*, et al.* (2007). The mitogen-activated protein kinase (MAPK)-activated protein kinases MK2 and MK3 cooperate in stimulation of tumor necrosis factor biosynthesis and stabilization of p38 MAPK. Molecular and cellular biology *27*, 170-181.

Ronkina, N., Kotlyarov, A., and Gaestel, M. (2008). MK2 and MK3--a pair of isoenzymes? Frontiers in bioscience : a journal and virtual library *13*, 5511-5521.

Russell, R.C., Tian, Y., Yuan, H., Park, H.W., Chang, Y.Y., Kim, J., Kim, H., Neufeld, T.P., Dillin, A., and Guan, K.L. (2013). ULK1 induces autophagy by phosphorylating Beclin-1 and activating VPS34 lipid kinase. Nature cell biology *15*, 741-750.

Seaman, M.N., Marcusson, E.G., Cereghino, J.L., and Emr, S.D. (1997). Endosome to Golgi retrieval of the vacuolar protein sorting receptor, Vps10p, requires the function of the VPS29, VPS30, and VPS35 gene products. The Journal of cell biology *137*, 79-92.

Shintani, T., Huang, W.P., Stromhaug, P.E., and Klionsky, D.J. (2002). Mechanism of cargo selection in the cytoplasm to vacuole targeting pathway. Developmental cell *3*, 825-837.

Shoji-Kawata, S., Sumpter, R., Leveno, M., Campbell, G.R., Zou, Z., Kinch, L., Wilkins, A.D., Sun, Q., Pallauf, K., MacDuff, D.*, et al.* (2013). Identification of a candidate therapeutic autophagy-inducing peptide. Nature *494*, 201-206.

Sithanandam, G., Latif, F., Duh, F.M., Bernal, R., Smola, U., Li, H., Kuzmin, I., Wixler, V., Geil, L., and Shrestha, S. (1996). 3pK, a new mitogen-activated protein kinase-activated protein kinase located in the small cell lung cancer tumor suppressor gene region. Molecular and cellular biology *16*, 868-876.

Smets, B., Ghillebert, R., De Snijder, P., Binda, M., Swinnen, E., De Virgilio, C., and Winderickx, J. (2010). Life in the midst of scarcity: adaptations to nutrient availability in Saccharomyces cerevisiae. Current genetics *56*, 1-32.

Stein, M., Lin, H., Jeyamohan, C., Dvorzhinski, D., Gounder, M., Bray, K., Eddy, S., Goodin, S., White, E., and Dipaola, R.S. (2010). Targeting tumor metabolism with 2-deoxyglucose in patients with castrate-resistant prostate cancer and advanced malignancies. The Prostate *70*, 1388-1394.

Stephan, J.S., Yeh, Y.Y., Ramachandran, V., Deminoff, S.J., and Herman, P.K. (2009). The Tor and PKA signaling pathways independently target the Atg1/Atg13 protein kinase complex to control autophagy. Proceedings of the National Academy of Sciences of the United States of America *106*, 17049-17054.

Stokoe, D., Engel, K., Campbell, D.G., Cohen, P., and Gaestel, M. (1992). Identification of MAPKAP kinase 2 as a major enzyme responsible for the phosphorylation of the small mammalian heat shock proteins. FEBS letters *313*, 307-313.

Sun, Q., Fan, W., Chen, K., Ding, X., Chen, S., and Zhong, Q. (2008). Identification of Barkor as a mammalian autophagy-specific factor for Beclin 1 and class III phosphatidylinositol 3-kinase. Proceedings of the National Academy of Sciences of the United States of America *105*, 19211-19216.

Szyniarowski, P., Corcelle-Termeau, E., Farkas, T., Hoyer-Hansen, M., Nylandsted, J., Kallunki, T., and Jaattela, M. (2011). A comprehensive siRNA screen for kinases that suppress macroautophagy in optimal growth conditions. Autophagy *7*, 892-903.

Tang, D., Kang, R., Livesey, K.M., Cheh, C.W., Farkas, A., Loughran, P., Hoppe, G., Bianchi, M.E., Tracey, K.J., Zeh, H.J., 3rd*, et al.* (2010). Endogenous HMGB1 regulates autophagy. The Journal of cell biology *190*, 881-892.

Tsukada, M., and Ohsumi, Y. (1993). Isolation and characterization of autophagy-defective mutants of Saccharomyces cerevisiae. FEBS letters *333*, 169-174.

Wang, R.C., Wei, Y., An, Z., Zou, Z., Xiao, G., Bhagat, G., White, M., Reichelt, J., and Levine, B. (2012). Akt-mediated regulation of autophagy and tumorigenesis through Beclin 1 phosphorylation. Science *338*, 956-959.

Wang, X., Pattison, J.S., and Su, H. (2013). Posttranslational modification and quality control. Circulation research *112*, 367-381.

Webber, J.L., and Tooze, S.A. (2010). New insights into the function of Atg9. FEBS letters *584*, 1319-1326.

Wei, W., Nurse, P., and Broek, D. (1993). Yeast cells can enter a quiescent state through G1, S, G2, or M phase of the cell cycle. Cancer research *53*, 1867-1870.

Wei, Y., Pattingre, S., Sinha, S., Bassik, M., and Levine, B. (2008). JNK1-mediated phosphorylation of Bcl-2 regulates starvation-induced autophagy. Molecular cell *30*, 678-688.

Wei, Y., Zou, Z., Becker, N., Anderson, M., Sumpter, R., Xiao, G., Kinch, L., Koduru, P., Christudass, C.S., Veltri, R.W.*, et al.* (2013). EGFR-mediated Beclin 1 phosphorylation in autophagy suppression, tumor progression, and tumor chemoresistance. Cell *154*, 1269-1284.

Weiss, E.L. (2012). Mitotic exit and separation of mother and daughter cells. Genetics *192*, 1165-1202.

Winzen, R., Kracht, M., Ritter, B., Wilhelm, A., Chen, C.Y., Shyu, A.B., Muller, M., Gaestel, M., Resch, K., and Holtmann, H. (1999). The p38 MAP kinase pathway signals for cytokine-induced mRNA stabilization via MAP kinase-activated protein kinase 2 and an AU-rich region-targeted mechanism. The EMBO journal *18*, 4969-4980.

Wirth, M., Joachim, J., and Tooze, S.A. (2013). Autophagosome formation--the role of ULK1 and Beclin1-PI3KC3 complexes in setting the stage. Seminars in cancer biology *23*, 301-309.

Yang, Z., Huang, J., Geng, J., Nair, U., and Klionsky, D.J. (2006). Atg22 recycles amino acids to link the degradative and recycling functions of autophagy. Molecular biology of the cell *17*, 5094-5104.

Yang, Z., and Klionsky, D.J. (2010). Eaten alive: a history of macroautophagy. Nature cell biology *12*, 814-822.

Yeong, F.M., Lim, H.H., Padmashree, C.G., and Surana, U. (2000). Exit from mitosis in budding yeast: biphasic inactivation of the Cdc28-Clb2 mitotic kinase and the role of Cdc20. Molecular cell *5*, 501-511.

Yi, C., Ma, M., Ran, L., Zheng, J., Tong, J., Zhu, J., Ma, C., Sun, Y., Zhang, S., Feng, W.*, et al.* (2012). Function and molecular mechanism of acetylation in autophagy regulation. Science *336*, 474-477.

Yue, Z., Jin, S., Yang, C., Levine, A.J., and Heintz, N. (2003). Beclin 1, an autophagy gene essential for early embryonic development, is a haploinsufficient tumor suppressor. Proceedings of the National Academy of Sciences of the United States of America *100*, 15077-15082.

Zalckvar, E., Berissi, H., Mizrachy, L., Idelchuk, Y., Koren, I., Eisenstein, M., Sabanay, H., Pinkas-Kramarski, R., and Kimchi, A. (2009). DAP-kinase-mediated phosphorylation on the BH3 domain of beclin 1 promotes dissociation of beclin 1 from Bcl-XL and induction of autophagy. EMBO reports *10*, 285-292.

Zetterberg, A., and Larsson, O. (1985). Kinetic analysis of regulatory events in G1 leading to proliferation or quiescence of Swiss 3T3 cells. Proceedings of the National Academy of Sciences of the United States of America *82*, 5365-5369.